

See discussions, stats, and author profiles for this publication at: <https://www.researchgate.net/publication/260060008>

# ChemInform Abstract: Conversion Reactions of Cadmium Chalcogenide Nanocrystal Precursors.

ARTICLE *in* CHEMISTRY OF MATERIALS · FEBRUARY 2013

Impact Factor: 8.35 · DOI: 10.1021/cm3035642

---

CITATIONS

29

---

READS

27

5 AUTHORS, INCLUDING:



Brandi M Cossairt

University of Washington Seattle

25 PUBLICATIONS 755 CITATIONS

SEE PROFILE



Haitao Liu

University of Pittsburgh

47 PUBLICATIONS 1,944 CITATIONS

SEE PROFILE

# Conversion Reactions of Cadmium Chalcogenide Nanocrystal Precursors

Raúl García-Rodríguez,<sup>†,||</sup> Mark P. Hendricks,<sup>‡,||</sup> Brandi M. Cossairt,<sup>\*,§</sup> Haitao Liu,<sup>\*,†</sup> and Jonathan S. Owen<sup>\*,‡</sup>

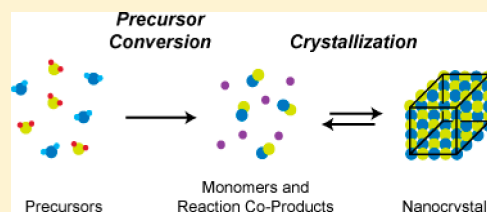
<sup>†</sup>Department of Chemistry, University of Pittsburgh, Pittsburgh, Pennsylvania 15260, United States

<sup>‡</sup>Department of Chemistry, Columbia University, New York, New York 10027, United States

<sup>§</sup>Department of Chemistry, University of Washington, Seattle, Washington 98195, United States

**ABSTRACT:** We survey the chemical reactions between common precursors used in the synthesis of metal chalcogenide nanocrystals and outline how they affect the mechanism and kinetics of nanocrystal growth. We emphasize syntheses of cadmium selenide and cadmium sulfide where a variety of metal and chalcogenide precursors have been explored, though this is supplemented by studies of zinc and lead chalcogenide formation where appropriate. This review is organized into three sections, highlighting kinetics, metal precursors, and chalcogenide precursors, respectively. Section I is dedicated to the role of precursor conversion as a source of monomers and the importance of the supply rate on nanocrystal nucleation and growth. Section II describes the structure and reactivity of cadmium carboxylates, phosphonates, and chalcogenolates. Section III describes the reaction chemistry of commonly employed chalcogenide precursors and the mechanisms by which they react with metal precursors.

**KEYWORDS:** II–VI, quantum dot, precursor conversion, cadmium chalcogenide, mechanism



## INTRODUCTION

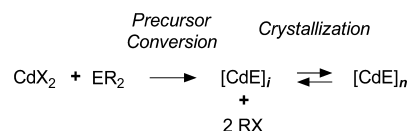
The synthesis of colloidal II–VI semiconductor nanocrystals relies on a chemical reaction between metal and chalcogenide precursors to form a material of interest. Though significant research has been devoted to the growth of the crystals themselves, only recently have the mechanisms and kinetics of reactions between precursors become a focus of study. These studies show that precursor reactivity can limit the rates of crystal nucleation and growth and are therefore key to synthetic reproducibility and scalability.

A deeper understanding of precursor reactions will clarify productive mechanistic pathways and the origin of their concentration dependence. Detailed knowledge of this kind is important to the design and synthesis of more complex nanocrystal geometries and compositions.<sup>1</sup> In addition, these studies will aid in the grand challenge of synthesizing nanocrystals with atomic precision, with the hope that complex inorganic systems may one day be understood and controlled much like small molecules. With these goals in mind it is clear that a more detailed look at precursor reactivity is greatly needed.

While the formation of colloidal crystals has been found to follow several mechanisms including autocatalytic<sup>2</sup> and aggregative processes,<sup>3–6</sup> many metal–chalcogenide nanocrystal syntheses appear to follow nucleation and growth pathways, where soluble monomers add to growing crystals or dissociate during Ostwald ripening. In these cases, nanocrystal syntheses can be viewed as two-step processes: first, a reaction between precursors supplies the reaction medium with

monomers ( $[\text{ME}]_i$ , Scheme 1) that subsequently undergo crystallization by assembly into nanocrystals ( $[\text{ME}]_n$ , Scheme

### Scheme 1. Precursor Conversion to Solute (Monomer) and Its Subsequent Crystallization to Nanocrystals



1). While crystallizations of these types have been the subject of several recent reviews,<sup>7–12</sup> the present manuscript focuses on the first step: the reaction between precursors.

Specifically, we survey the chemical reactions between common precursors used in the synthesis of metal chalcogenide nanocrystals and outline how they affect the mechanism and kinetics of nanocrystal growth. We emphasize syntheses of cadmium selenide and cadmium sulfide where a variety of metal and chalcogenide precursors have been explored, though this is supplemented by studies of zinc and lead chalcogenide formation where appropriate. While a significant portion of the information contained in the review is drawn from the

**Special Issue:** Synthetic and Mechanistic Advances in Nanocrystal Growth

**Received:** November 4, 2012

**Revised:** January 22, 2013

nanocrystal literature, many of the mechanistic insights derive from studies conducted under related reaction conditions.

This review is organized into three sections, highlighting kinetics, metal precursors, and chalcogenide precursors, respectively. Section I is dedicated to the role of precursor conversion as a source of monomers and the importance of the supply rate on nanocrystal nucleation and growth. Section II describes the structure and reactivity of cadmium carboxylates, phosphonates, and chalcogenolates. Finally, Section III describes the reaction chemistry of commonly employed chalcogenide precursors and the mechanisms by which they react with metal precursors.

## SECTION I: PRECURSOR REACTION KINETICS AND CRYSTALLIZATION

In colloidal nanocrystal syntheses, precursor reactions precede the crystallization steps and are often irreversible, meaning that to a first approximation the conversion rate is not affected by the concentration of monomer or nanocrystal products.<sup>13</sup> In this scenario, precursors can be thought of as an internal reservoir of monomers that are released by the conversion reaction. In many cases the conversion process is slower than the consumption of monomers by growth and limits the rate of crystallization. For example, in crystallization reactions that follow the La Mer model of colloidal crystallization, the precursor reaction determines the rate at which monomers supersaturate prior to nucleation (Phase I, Figure 1).<sup>14</sup> Early investigations of colloidal crystallization utilized the rate of these reactions to control crystal nucleation and growth.<sup>15</sup>

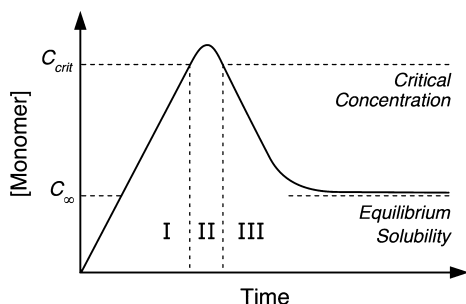


**Figure 1.** Kinetics of solute supersaturation according to La Mer.<sup>14</sup> Three phases of the La Mer model include (I) supersaturation, (II) nucleation, and (III) growth. Precursor conversion reactions that limit the crystallization determine the temporal evolution of monomer concentration as well as the steady state supersaturation during the growth phase.

**Conversion Kinetics and Nanocrystal Nucleation and Growth.** A number of experimental and theoretical studies have examined the influence of monomer supply kinetics on nucleation and growth.<sup>16–20</sup> In these studies the monomer supply rate controls the number of crystals produced during the nucleation phase and can be used to tune the nanocrystal diameter. Sugimoto et al. proposed a model to explain this result that divides the consumption of monomer produced during the nucleation phase ( $QV_m$ ,  $Q$  = molar production rate,  $V_m$  = molar volume) into two components: (1) the production of nuclei ( $v^*(dn/dt)$ ,  $n$  = number of nuclei,  $v^*$  = nucleus volume) and (2) their growth ( $vn_t$ ,  $v$  = average nucleus growth rate,  $n_t$  = number of nuclei at time  $t$ ).<sup>16</sup> Assuming that the concentration of monomer changes minimally during the nucleation phase, the growth rate of nuclei ( $v$ ) will be a

constant and eq 1 can be integrated over the nucleation phase. This simplification suggests the final number of nuclei ( $n_t$ ) is proportional to the rate of monomer generation during nucleation.

$$Q_0V_m = v^*\frac{dn}{dt} + vn_t \quad (1)$$

$$n_t = \frac{Q_0V_m}{v} \quad (2)$$

While Sugimoto et al. demonstrated the relationship between supply rate and nucleation by controlled mixing of silver and chloride or bromide ions, several experimental studies on II–VI metal chalcogenides observed a similar relationship by adjusting precursor concentrations. These include reactions of tri-*n*-octylphosphine selenide with cadmium phosphonate,<sup>20</sup> cadmium carboxylate,<sup>21,22</sup> and amine/carboxylate mixtures.<sup>19,23</sup> By measuring the precursor conversion rate during nucleation ( $Q_0$ ) and comparing it with the number of nanocrystals produced by nucleation ( $n_t$ ), a nearly linear relationship was observed (Figure 2).<sup>20</sup> Under these conditions the rate increased with

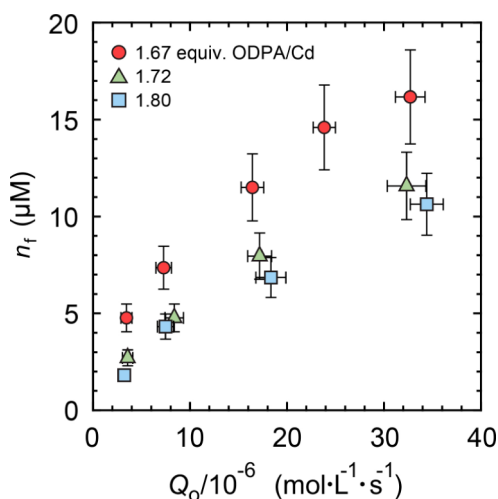


**Figure 2.** Final nanocrystal concentration ( $n_t$ ) versus initial precursor conversion rate ( $Q_0$ ) across three concentrations of octadecylphosphonic acid (1.67 equiv, red circles; 1.72 equiv, green triangles; 1.80 equiv, blue squares) Reproduced with permission from ref 20. Copyright 2010 American Chemical Society.

precursor concentration in a second order fashion. A similar conclusion was reached by analyzing the nanocrystal concentrations produced by a series of phosphine chalcogenides with different structures and conversion rates.

Several theoretical studies have examined the effect of precursor-to-monomer conversion kinetics on the outcome of a nanocrystals synthesis. Abe et al. simulated the temporal evolution of nanocrystals during growth by combining a first-order monomer supply rate with classical nucleation theory. Their simulations showed that both the concentration of nanocrystals and their diameter can be adjusted by the rate of monomer supply (Figure 3).<sup>19</sup>

Monomer supply kinetics also influences nanocrystal growth by maintaining the supersaturation after nucleation. Supersaturation is known to influence the size distribution and shape evolution of the nanocrystal products.<sup>7,24</sup> Rempel et al. and Clark et al. developed models that analyze the influence of monomer production on size distribution focusing and

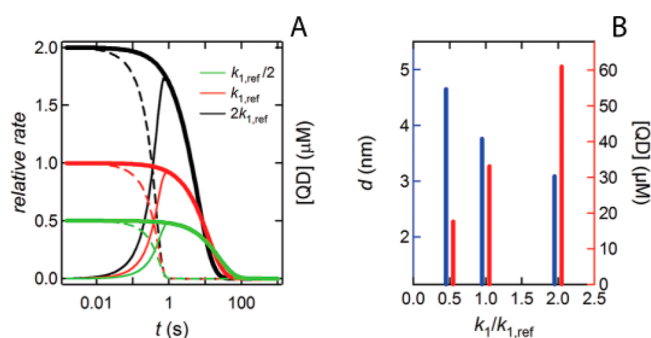


**Figure 3.** (a) Effect of monomer generation rate (bold lines) on the rate of monomer consumption by nucleation (dotted lines) and growth (full lines). (b) Effect of monomer generation rate on the nanocrystal diameter (blue) and concentration (red) at the end of the focusing regime. The simulation assumes first order kinetics for the monomer generation reaction. Reproduced with permission from ref 19. Copyright 2012 American Chemical Society.

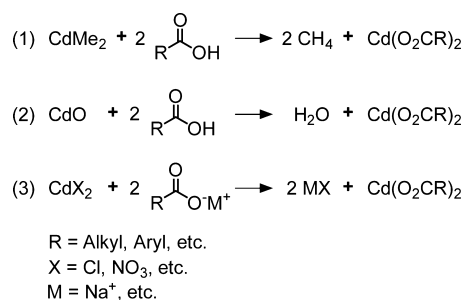
broadening. Their models show that when the balance between monomer production and consumption maintains a high supersaturation during growth, nanocrystals undergo size-distribution focusing, while at low supersaturation, Ostwald ripening becomes important.<sup>18,25</sup> In addition, early proposals on the kinetic origins of anisotropic growth suggest that high steady-state monomer concentrations are essential to maximizing the aspect ratio of CdSe nanorods.<sup>26</sup> Recent investigations by Wang and Buhro<sup>27</sup> and Vela et al.<sup>28</sup> demonstrate that tuning the precursor conversion rate can influence the aspect ratio of rod-shaped nanocrystals and support mechanisms where anisotropic growth is assisted by a smaller number of nanocrystals.

**Effect of Surfactants on Nucleation.** Several studies have documented a relationship between the concentration of surfactants and nanocrystal size, with higher concentrations of oleic,<sup>22,29–31</sup> phosphonic,<sup>20</sup> and phosphinic acid<sup>30</sup> producing lower concentrations of nanocrystals. While early studies suggest surfactants inhibit nucleation by coordinating the starting cadmium ions and reducing their reactivity, it was later shown that phosphonic acids have a negligible effect on the precursor conversion rate and yet a substantial impact on the particle size;<sup>20</sup> these authors proposed that phosphonic acids increase the rate at which nuclei grow during the nucleation phase, thereby decreasing the final number of nanocrystals ( $n_b$ , eq 2). In support of this hypothesis, phosphonic acids were shown to catalyze Ostwald ripening, which may provide a mechanism by which nuclei grow in the presence of acid. Similarly, in their studies of CdSe growth Dushkin and co-workers proposed that carboxylic acids cause “early-time ripening” to explain the relationship between average nanocrystal size and carboxylic acid concentration.<sup>22</sup>

## SECTION II: PREPARATION, STRUCTURE, AND REACTIVITY PATTERNS OF CADMIUM PRECURSORS USED IN CADMIUM CHALCOGENIDE NANOCRYSTAL SYNTHESIS

**Part IIA: Cadmium Carboxylates.** Carboxylate complexes of cadmium are common nanocrystal precursors and can be prepared in a number of ways as shown in Scheme 2. Most commonly, the reaction of carboxylic acids (2 equiv) with CdO, Cd(O<sub>2</sub>CMe)<sub>2</sub>, or CdMe<sub>2</sub> generates cadmium carboxylate and water, acetic acid, or methane byproducts. These cadmium

### Scheme 2. Methods for the Preparation of Cadmium Carboxylates



carboxylates are then typically used in situ, sometimes after degassing, without further workup or purification. Alternatively, metal carboxylates may be prepared from the reaction of an alkali metal carboxylate with a cadmium salt, such as cadmium chloride or cadmium nitrate.<sup>32</sup> These reactions are typically run in aqueous solution or in the presence of alcohols, making drying key to their purification. Water often associates with cadmium complexes as an adduct or by forming a hydroxide.<sup>33</sup> Indeed, a search of cadmium carboxylates in the Cambridge Structural Database shows that the large majority of known structures have water molecules bound to the cadmium center. Similarly, the remaining acetic acid can affect the reaction outcome.<sup>34,35</sup>

The versatility of the RCO<sub>2</sub><sup>−</sup> ligand is reflected in the variety of metal binding modes it can adopt (Figure 4). Cd<sup>2+</sup> can

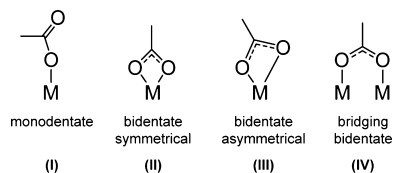


**Figure 4.** Coordination motifs of carboxylate to metal ions.

accommodate a great variety of structural arrangements about the metal center, including structures where the metal center is displaced from the plane defined by the bound O=C–O fragment by as much as 1.5 Å;<sup>32</sup> other metal ions tend to lay in the carboxylate plane with little to no deviation.

Examples of this structural flexibility can be observed in crystal structures of Cd(O<sub>2</sub>CPh)<sub>2</sub>, Cd(O<sub>2</sub>CMe)(O<sub>2</sub>CPh)·(H<sub>2</sub>O), and others, all of which are extended one-dimensional coordination polymers.<sup>32</sup> In structures containing water molecules, extensive hydrogen bonding networks lead to additional structural complexity. In the solution phase it has been found that metal carboxylates with aliphatic carboxylate ligands form micellar structures at concentrations as low as 10<sup>−4</sup> M in nonaqueous media.<sup>33</sup> The number of molecules per micelle has been shown to increase as the acid chain length decreases.<sup>33</sup> The structure of the cadmium precursor, be it polymeric, molecular, or some mixture of these, can affect the kinetics of nanocrystal reactions and lead to synthetic irreproducibility if not properly controlled.<sup>36</sup>

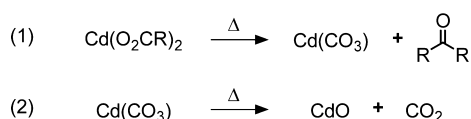
Assigning the coordination modes of carboxylate to metal centers has been studied in detail using infrared spectroscopy.<sup>37</sup> Carboxylates typically take on one of three structures: monodentate (I), chelating bidentate (II and III), and bridging bidentate (IV) (Figure 4). The carbonyl stretching bands in cadmium alkylcarboxylate complexes with alkyl chains ranging



in length from 1 to 18 carbon atoms span a very narrow range for both the symmetric ( $1540\text{--}1548\text{ cm}^{-1}$ ) and the antisymmetric stretch ( $1408\text{--}1414\text{ cm}^{-1}$ ). Interestingly, the antisymmetric  $\text{COO}^-$  stretching frequency is quite high in cadmium carboxylates (especially when compared to the analogous zinc and lead compounds). This data collectively suggests that carboxylate binds  $\text{Cd}^{2+}$  in an asymmetric chelating bidentate binding geometry (structure III)<sup>38</sup> and is not affected by its aliphatic chain length.

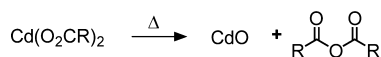
The thermal decomposition of hydrated and anhydrous cadmium carboxylates has been studied both in inert atmosphere and under ambient conditions. Solid cadmium carboxylates are known to decompose above  $200\text{ }^\circ\text{C}$ , eventually leading to the formation of  $\text{CdO}$ .<sup>39,40</sup> The decomposition of cadmium acetate in an inert atmosphere, for example, becomes significant around  $250\text{ }^\circ\text{C}$ , where acetone begins to evolve and cadmium carbonate is formed (Scheme 3). By  $280\text{ }^\circ\text{C}$ , all of the acetone has evolved and  $\text{CO}_2$  begins to eliminate from cadmium carbonate leaving  $\text{CdO}$ ; similar trends are observed in an oxidizing atmosphere.<sup>41</sup>

**Scheme 3. Decomposition of Cadmium Carboxylate at Elevated Temperature**



Decomposition of cadmium carboxylates to cadmium oxide and the corresponding acid anhydride is also observed and may be catalyzed by acid (Scheme 4).<sup>32,40</sup> The temperature at which

**Scheme 4. Alternative Thermal Decomposition Pathway for Cadmium Carboxylate**



cadmium carboxylates decompose in the solid state coincides with the reaction temperatures at which many colloidal nanocrystal syntheses are run. Thus, the intermediacy of  $\text{CdO}$  and  $\text{Cd}(\text{CO}_3)$  may play an important role in precursor conversion. Indeed,  $\text{CdO}$  and  $\text{Cd}(\text{CO}_3)$  are known precursors to  $\text{CdE}$  nanocrystals.<sup>42</sup> Although this reactivity has not been studied in detail under nanocrystal synthesis conditions, the presence of multiple cadmium precursors generated by partial decomposition to  $\text{CdO}$  or  $\text{Cd}(\text{CO}_3)$  is likely to cause multiple reaction pathways and thus ill-defined conversion kinetics. This will be further complicated by the presence of additional carboxylic acids or amines, which can influence the decomposition path.<sup>23,42,43</sup>

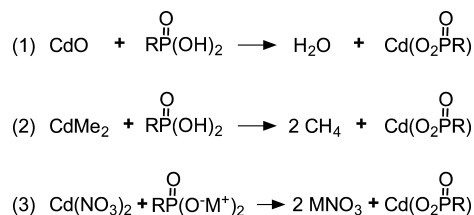
Cadmium carboxylates can accept a wide variety of neutral donor ligands including amines, pyridines, pyrroles, and phosphines. Binding of one neutral donor ligand to the cadmium center is generally insufficient to break up the coordination polymer structure; however, binding two donors results in the formation of discrete mononuclear molecular species.<sup>44</sup> Kinetic studies suggest that the nature of the carboxylate group has significant effects on the composition of the donor–cadmium carboxylate complexes and on the rate constant and activation energy of the ligand binding process.<sup>32</sup> The binding of neutral donors to cadmium carboxylates may alter their inherent reactivity during nanocrystal syntheses by

changing their extent of polymerization, morphology, and acidity, as well as the solution viscosity.

**Part IIB: Cadmium Phosphonates.** The seminal synthesis of  $\text{CdSe}$  nanocrystals published by Murray, Norris, and Bawendi involved the reaction of  $\text{CdMe}_2$  with tri-*n*-octylphosphine selenide ( $\text{TOPSe}$ ) in molten tri-*n*-octylphosphine oxide ( $\text{TOPO}$ ).<sup>45</sup> After that initial report, the realization that acidic impurities in  $\text{TOPO}$  (e.g., phosphonic and phosphinic acids)<sup>46</sup> were responsible for controlling nanocrystal growth led Peng et al. to develop synthetic methods that utilized phosphonic acids and  $\text{CdMe}_2$ ,<sup>47</sup> and later combinations of cadmium oxide and phosphonic acids<sup>48</sup> to synthesize  $\text{CdSe}$  nanocrystals. From these investigations, it was determined that the cadmium phosphonate precursor binds the nanocrystal product resulting in a metal-rich composition with anionic phosphonate surface termination.<sup>49–53</sup> A similar conclusion has been reached for cadmium carboxylate.<sup>34,54–56</sup> The success of methods developed by Peng has led many researchers to use cadmium phosphonate precursors formed either in situ or as isolated materials.

Metal phosphonates are readily prepared by reaction of a metal salt with a desired phosphonic acid. For example,  $\text{Cd}(\text{O}_3\text{PR})_2 \cdot \text{H}_2\text{O}$  ( $\text{R} = \text{CH}_3, \text{C}_6\text{H}_5$ ) is prepared by combining  $\text{Cd}(\text{NO}_3)_2 \cdot 4\text{H}_2\text{O}$  with an equimolar aqueous solution of the phosphonic acid, followed by a basic workup with  $\text{NaOH}$  (Scheme 5).<sup>57</sup> Cadmium phosphonates can also be prepared by

**Scheme 5. Methods for the Preparation of Cadmium Phosphonates**



combining dialkyl cadmium with phosphonic acids, releasing methane. This latter procedure is a convenient method to prepare anhydrous cadmium alkylphosphonates in situ.<sup>20,45,50,58</sup> Preparation of cadmium alkylphosphonates from cadmium oxide is complicated by the formation of water, which can be difficult to remove and is known to accelerate the precursor conversion rate.<sup>34</sup>

Depending on reaction stoichiometry, mixed phosphonate/monohydrogen phosphonate oligomers can be obtained.<sup>59</sup> For example, 2,4,6-triisopropylphenylphosphonic acid can be treated with  $\text{Cd}(\text{OAc})_2 \cdot 2\text{H}_2\text{O}$  in a 1:1 ratio in methanol to give the tetrameric  $\text{Cd}_4(\text{ArPO}_3)_2(\text{ArPO}_3\text{H})_4(\text{CH}_3\text{OH})_4$  (Figure 5). This tetrameric arrangement of cadmium atoms can also be obtained as an adduct of dimethylformamide.

Cadmium alkyl and aryl phosphonates were first structurally characterized by Cao et al. in 1993.<sup>60</sup> Both  $\text{Cd}(\text{O}_3\text{PCH}_3)_2 \cdot \text{H}_2\text{O}$  and  $\text{Cd}(\text{O}_3\text{PC}_6\text{H}_5)_2 \cdot \text{H}_2\text{O}$  have similar structures with layers of  $\text{Cd}(\text{O}_3\text{PR})_2 \cdot \text{H}_2\text{O}$  units that stack along the *a* axis and are separated by their methyl or phenyl substituents. Separation by the organic substituents leads to van der Waals interactions between the layers. The cadmium atoms are located approximately in the midpoint of the layer and are octahedrally coordinated by five oxygen atoms of phosphonate groups and a water molecule (Figure 6).

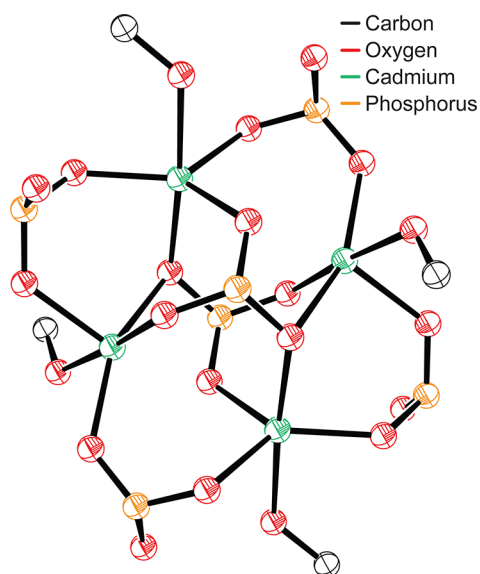


**Figure 5.** Crystal structure of  $\text{Cd}_4(\text{ArPO}_3)_2(\text{ArPO}_3\text{H})_4(\text{CH}_3\text{OH})_4$ . Aryl groups and hydrogen atoms omitted for clarity.

The same lamellar structure was observed in crystal structures of Mn, Zn, Co, and Mg phenyl and alkyl phosphonates.<sup>57</sup> The metals are six-coordinate, with two chelating phosphonate oxygen atoms that also bridge adjacent metal centers. These three-coordinate oxygen atoms are situated above and below the mean plane of the layer. A fifth coordination site is filled by the third phosphonate oxygen atom that connects the rows of metal atoms along the *a* axis to create the layer. A water molecule occupies the sixth site in these structures. As first recognized by Clearfield et al., some divalent metal phosphonates have structures related to inorganic metal phosphates. For example,  $\text{M}^{\text{II}}(\text{O}_3\text{PCH}_3)_2\cdot\text{H}_2\text{O}$  ( $\text{M}^{\text{II}} = \text{Co, Mg, Mn, Ni, Zn}$ ) are similar to  $\text{M}^{\text{I}}\text{M}^{\text{II}}(\text{PO}_4)_2\cdot\text{H}_2\text{O}$  ( $\text{M}^{\text{I}} = \text{NH}_4$ ,  $\text{M}^{\text{II}} = \text{Cd, Co, Fe, Mg, Mn, Ni}$ ;  $\text{M}^{\text{I}} = \text{K}$ ,  $\text{M}^{\text{II}} = \text{Cd, Co, Mg, Mn, Ni}$ ).<sup>60</sup>

Other, more complex, oligomers of cadmium phosphonate have been structurally characterized. The largest of such aggregates was prepared by Roesky et al. in 2003 from *tert*-butylphosphonic acid.<sup>61</sup> In their preparation,  $[(\text{MeCd})_{10}((\text{THF})\text{Cd})_4\text{Cd}_6(\mu_4\text{-O})_2(\mu_3\text{-OH})_2(\text{tBuPO}_3)_{12}]$  is obtained through the dropwise addition of dimethyl cadmium to a solution of *tert*-butylphosphonic acid in a 2:1 ratio at room temperature (Figure 7). The difference between this structure and other alkylphosphonates may stem for the steric encumbrance of the *tert*-butyl substituent; nonetheless, cadmium phosphonates take on a variety of oligomeric structures that may lead to variability during nanocrystal synthesis. In fact, Peng and Peng have shown that cadmium phosphonate precursors change in composition as they “age” leading to significant differences in the shape of the resultant

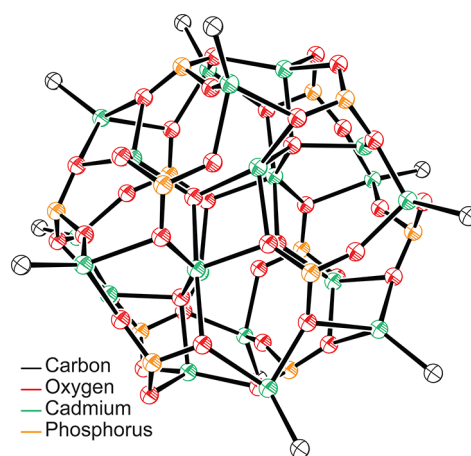


**Figure 7.** Crystal structure of  $[(\text{MeCd})_{10}((\text{THF})\text{Cd})_4\text{Cd}_6(\mu_4\text{-O})_2(\mu_3\text{-OH})_2(\text{tBuPO}_3)_{12}]$ . THF, tBu, and hydrogen atoms omitted for clarity.

$\text{CdSe}$  nanorod.<sup>26</sup> In addition, the solubility of anhydrous cadmium octadecylphosphonate in TOPO and the viscosity of reaction mixture depends on the number of phosphonic acids per cadmium, a result that was explained by a change in the structure of a polymeric cadmium complex.<sup>20</sup>

Thermogravimetric studies have shown that  $[\text{Cd}(\text{O}_2\text{PCH}_3)_2\cdot\text{H}_2\text{O}]$  dehydrates beginning around 150 °C.<sup>57</sup> In many nanocrystal syntheses excess phosphonic acid is used, leading to  $\text{Cd}(\text{HO}_2\text{PCH}_3)_2$  complexes.<sup>34</sup> Although bisphosphonates of cadmium have been studied less, it is known that they dehydrate at temperatures below 500 °C, eventually producing a phosphonate anhydride complex of cadmium.<sup>57</sup> Phosphonic anhydrides are also byproducts of the reaction between TOPSe and cadmium alkylphosphonates and have been identified on the surfaces of  $\text{CdSe}$  nanocrystals.<sup>46,49,50</sup>

Similarly, primary amine adducts of cadmium phosphonates also undergo thermal desorption. For example,  $[\text{Cd}(\text{O}_2\text{PCH}_3)_2(\text{H}_2\text{NC}_{10}\text{H}_{21})]_n$  loses dodecylamine beginning around 200 °C.<sup>60</sup> The layered structure of  $\text{M}^{\text{II}}(\text{O}_3\text{PCH}_3)_2$  ( $\text{M}^{\text{II}} = \text{Zn, Co}$ ) intercalates primary amines and ammonia leading to a new interlayer spacing that depends on the amine chain length (1.2913 Å/CH<sub>2</sub>), and such behavior has led to many applications in shape-selective chemical sensing.<sup>62</sup> Unlike Zn and Co, cadmium organophosphonates intercalate amines both from the vapor and solution phase.<sup>60</sup> The intercalation of primary amines into cadmium phosphonate polymers was found to approach equilibrium in solution (1 Cd: 1 H<sub>2</sub>NR) after 3–5 days, while the initial reaction rate is fast. For example, 0.5 g of  $\text{Cd}(\text{O}_3\text{PCH}_3)_2$  suspended in acetonitrile containing 1 g of dodecylamine for 15 min afforded a single solid phase with a stoichiometry of  $\text{Cd}(\text{O}_3\text{PCH}_3)_2(\text{C}_{12}\text{H}_{25}\text{NH}_2)_{0.725}$ .<sup>60</sup>

**Part IIC: Cadmium Chalcogenolates.** Much like the other cadmium precursors,  $\text{Cd}(\text{ER})_2$  ( $\text{E} = \text{S, Se, Te}$ ) can be prepared

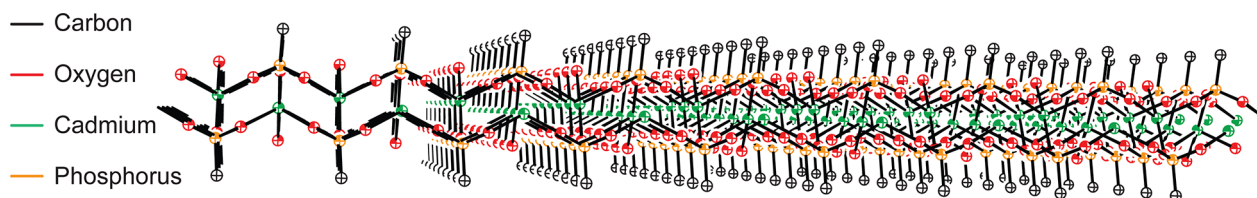
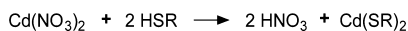


**Figure 6.** Crystal structure of  $\text{Cd}(\text{O}_3\text{PCH}_3)_2\cdot\text{H}_2\text{O}$ . Hydrogen atoms omitted for clarity.

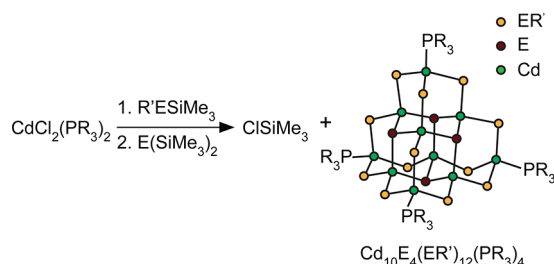
from an appropriate cadmium salt, such as  $\text{Cd}(\text{NO}_3)_2 \cdot 4\text{H}_2\text{O}$  or  $\text{CdCl}_2$ , and the desired chalcogenol or chalcogenolate anion (Scheme 6,  $\text{E} = \text{S}$ ).<sup>63–66</sup> Even in the presence of added triethylamine, DMF, and/or methanol, solid  $\text{Cd}(\text{ER})_2$  is typically isolated without coordinated solvent molecules.<sup>64</sup>

#### Scheme 6. Conversion of Cadmium Nitrate to Cadmium Thiolate



Many molecular, nonstoichiometric cadmium chalcogenide clusters have been prepared from cadmium chalcogenolate precursors. Typically, they are synthesized by combining  $\text{CdCl}_2(\text{PR}_3)_2$  with  $\text{R}'\text{ESiMe}_3$  and  $\text{E}(\text{SiMe}_3)_3$  ( $\text{E} = \text{S}, \text{Se}$ ) in an appropriate ratio and in the presence of an ammonium chloride salt when anionic clusters are desired (Scheme 7). This generalized procedure has been used to prepare  $\text{Cd}_4$ ,  $\text{Cd}_{10}$ ,  $\text{Cd}_{17}$ ,  $\text{Cd}_{32}$ , and  $\text{Cd}_{54}$  clusters.<sup>67,68</sup>

#### Scheme 7. Reaction of Cadmium Chloride Phosphine Complex with $\text{E}(\text{SiMe}_3)_2$ and $\text{R}'\text{ESiMe}_3$



The earliest group XII  $\text{M}(\text{ER})_2$  complex [ $\text{Zn}_4(\text{SPh})_8(\text{MeOH})$ ] was crystallized and shown to be composed of adamantanoid cages of [octahedro- $(\mu\text{-SPh})_6$ -tetrahedro- $\text{Zn}_4$ ] linked by  $\mu_2\text{-PhS}^-$  ligands, with terminal  $\text{PhS}^-$  and  $\text{MeOH}$  ligands at the other two Zn atoms.<sup>69</sup>  $\text{Cd}(\text{SPh})_2$  and  $\text{Cd}(\text{SC}_6\text{H}_4\text{Me-4})_2$  were first structurally characterized by Dance et al. and form similar, three-dimensional coordination polymers with adamantanoid cages linked by thiolate bridges as shown in Figure 8.<sup>64</sup> Such linked adamantanoid structures are ubiquitous for  $\text{Cd}(\text{ER})_2$  species and are analogous to zeolite

alumino-silicates due to their extended and open networks (Figure 8, right).

Due to their polymeric structure, cadmium chalcogenoates are typically insoluble in most organic solvents. Some of these compounds are, however, soluble in dimethylformamide and dissolve in the presence of stoichiometric amounts of bidentate neutral donors, such as tetramethylethylenediamine, phenanthroline, and bipyridine, or an excess of a monodentate donor, such as primary amine.<sup>70</sup> Interestingly, cadmium chalcogenoates undergo a number of insertion reactions, an example of which is the insertion of  $\text{CS}_2$  to make the corresponding  $\text{Cd}(\text{S}_2\text{CSR})_2$  complexes.<sup>70</sup>

It was observed quite early on that cadmium chalcogenolates decompose at high temperature ( $>250^\circ\text{C}$ ) to give bulk and nanostructured  $\text{CdE}$  ( $\text{E} = \text{S}, \text{Se}$ ) semiconductor materials.<sup>71,72</sup> More recently it has been shown that nonstoichiometric cadmium chalcogenolate clusters can undergo thermal decomposition at mild temperatures ( $\sim 60^\circ\text{C}$ ) in the presence of primary amine to give monodisperse nanocrystals<sup>73</sup> and in the presence of transition metal ( $\text{TM}^{2+}$ ) salts leading to TM-doped nanocrystals.<sup>74</sup> It remains an interesting question whether or not these  $\text{CdE}$  adamantoid clusters dissolve en route to nanocrystal formation, or whether they can act as nuclei or a template for particle growth.<sup>73</sup> Nevertheless, metal chalcogenolates are among the most widely used of the single-source precursors for the preparation of cadmium chalcogenide nanocrystals. Many other single-source precursors have been discovered, and their chemistry has been reviewed elsewhere.<sup>75,76</sup>

**Part IID: Effect of Cadmium Precursor on Nanocrystal Growth: Morphology Control.** As described in Sections IIA–IIC, the precise structure and composition of cadmium carboxylate, phosphonate, and chalcogenolate precursors can vary considerably depending on the preparation conditions. This diversity in structure has important implications for nanocrystal syntheses, particularly in studies where these precursors are formed in situ. Several studies on shape control, for example, have shown the importance of acid concentration (e.g., phosphonic or carboxylic acids) to the final size and shape.<sup>27</sup> Peng et al. have described the elongation of dots into rods using low concentrations of hexylphosphonic acid. Mixtures of hexylphosphonic acid (1.5–3 wt %) in TOPO generate monodisperse spherical nanocrystals, while higher

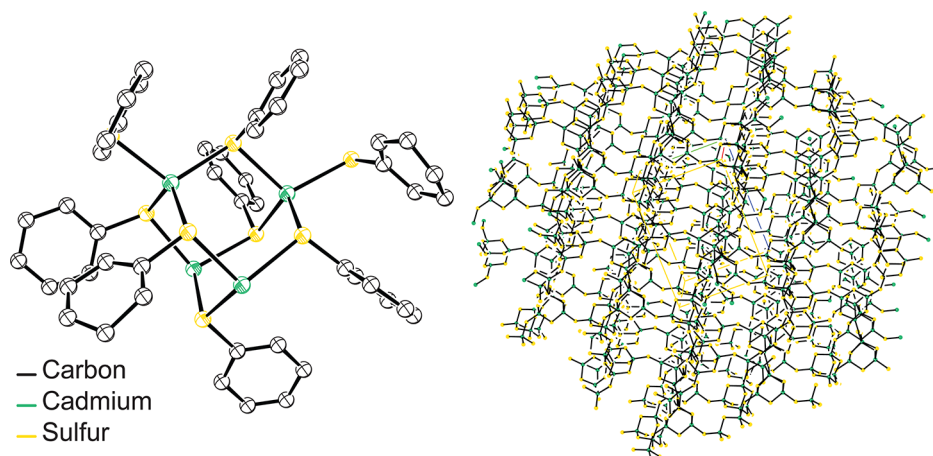


**Figure 8.** Crystal structure of  $\text{Cd}(\text{SPh})_2$ . Left: Asymmetric unit, hydrogen atoms omitted for clarity. Right: Extended solid state structure, phenyl groups and hydrogen atoms omitted for clarity.



concentrations (5–20 wt %) in TOPO reproducibly give rod structures.<sup>47</sup> Many explanations for the origin of this change in growth kinetics have been proposed, including the selective binding of phosphonic acids to rod walls, discouraging growth along those faces.<sup>77</sup> However, change in the structure of the cadmium phosphonate precursor may also be important.

The extended structure of cadmium precursors can also impact the morphology of the resulting product through a soft templating effect. For example, Hyeon and co-workers have shown that 2D CdSe nanosheets are formed from  $\text{CdCl}_2(\text{H}_2\text{NR})_2$  which has a lamellar structure enforced by van der Waals attraction between the alkyl side chains of the primary amine.<sup>78</sup> Similarly Buhro and co-workers have shown that  $\text{Cd}(\text{OAc})_2$  forms a lamellar structure in the presence of long-chain primary amines that templates the assembly of  $(\text{CdSe})_{13}$  nanoclusters into 2D quantum belts.<sup>79</sup> These examples clearly highlight the importance of cadmium precursor structure and its effect on nanocrystal syntheses.

### SECTION III: PREPARATION, STRUCTURE, AND REACTIVITY PATTERNS OF CHALCOGENIDE PRECURSORS USED IN CADMIUM CHALCOGENIDE NANOCRYSTAL SYNTHESIS

**Part IIIA: Tertiary Phosphine Chalcogenides.** Tertiary phosphine chalcogenides ( $\text{R}_3\text{PE}$ ) were among the first chalcogenide sources used in colloidal nanocrystal syntheses and remain one of the most common precursors.<sup>45</sup> Their popularity results from their ease of preparation, high solubility, and desirable reactivity in many organic solvents.<sup>42,80</sup> Simply combining a tertiary phosphine with elemental sulfur and selenium either in an inert solvent or neat leads to its conversion to the desired phosphine chalcogenide;<sup>81</sup> although tri-*n*-alkylphosphine sulfide and selenides are frequently described as a “solution” of chalcogen in phosphine, there is no free elemental chalcogen in the final reaction product. Instead, chemical oxidation of the phosphine occurs, either rapidly in the case of  $\text{R}_3\text{PS}$  or after several hours in the case of  $\text{R}_3\text{PSe}$ .<sup>82</sup> Oxidation of the phosphine is known to proceed without inversion of the phosphorus atom.<sup>83</sup> In addition to this direct approach, several other methods have been reported; however, they are seldom used due to their complexity relative to the direct approach.<sup>84–86</sup> Many nanocrystal reactions utilize a mixture of the phosphine chalcogenide and its parent phosphine, which has been shown to influence the rate of nanocrystal formation.<sup>87</sup>

Tertiary phosphine tellurides are often prepared in an analogous fashion; however, an equilibrium between the phosphine telluride and elemental tellurium is established (within hours) that depends on the phosphine substituents (Scheme 8).<sup>81,88,89</sup> This equilibrium makes pure trialkyl and triaryl phosphine tellurides unstable. However, tri-*n*-alkylphosphine tellurides can be isolated by selective precipitation, though they slowly eliminate elemental tellurium when stored

as solids at  $-78^\circ\text{C}$  and in solution where tellurium mirrors are sometimes formed.<sup>81,90</sup>

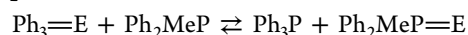
**Structure.** X-ray crystallography, infrared, and NMR spectroscopic studies show that tertiary phosphine chalcogenides are quasi-tetrahedral phosphorus complexes and that the phosphorus–chalcogen bond length is between that of the corresponding single and double bonds.<sup>91</sup> Both doubly bonded and singly bonded ylide resonance depictions are common, with the singly bonded structure becoming more important as one descends the period<sup>92</sup> leading to an increasing dipole moment  $^+\text{P}-\text{S}^- < ^+\text{P}-\text{Se}^- < ^+\text{P}-\text{Te}^-$ .<sup>84,93</sup> As shown in Table 1, the bond dissociation energy of  $\text{P}=\text{E}$ , as measured by calorimetry, decreases as one descends the period ( $\text{P}-\text{S} > \text{P}-\text{Se} > \text{P}-\text{Te}$ ).<sup>82</sup>

**Table 1. Bond Dissociation Energy (BDE) of  $\text{P}=\text{E}$ <sup>82</sup>**

compound	$\text{E}=\text{P}$ (BDE) (kcal/mol)
$\text{Bu}_3\text{P}=\text{S}$	96
$\text{Ph}_3\text{P}=\text{S}$	88
$\text{Bu}_3\text{P}=\text{Se}$	75
$\text{Ph}_3\text{P}=\text{Se}$	67
$\text{Bu}_3\text{P}=\text{Te}$	52

**Reactivity.** Most tertiary phosphine sulfides and selenides are thermally robust,<sup>84</sup> whereas the tertiary phosphine tellurides are not, some of which decompose to release metallic tellurium well below room temperature.<sup>81</sup> Exposure to air or gentle warming also causes decomposition.<sup>81</sup> This trend in stability is also reflected in the rate of chalcogenide exchange between free tertiary phosphine and  $\text{R}_3\text{PE}$ , exemplified in the kinetics study of the reaction series shown in Table 2.<sup>94</sup> Chalcogenide

**Table 2. Data for the Equilibrium between  $\text{Ph}_3\text{P}=\text{E}$  and  $\text{Ph}_2\text{MeP}$**

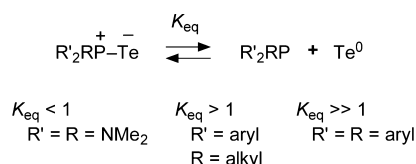


E	temp ( $^\circ\text{C}$ )	$K_{\text{eq}}$	$t_{1/2}$ (s)
O	250		>30 000
S	130	12	530
Se	30	22	<2

exchange between phosphine chalcogenides and their parent phosphines (i.e., self-exchange) is fast on the NMR time scale for phosphine tellurides.<sup>95,96</sup> Due to the relative weakness of the  $\text{P}-\text{Se}$  and  $\text{P}-\text{Te}$  bond,  $\text{R}_3\text{PSe}$  and  $\text{R}_3\text{PTe}$  are often more reactive sources of chalcogen than the elemental forms.<sup>84</sup>

The donor property of tertiary phosphine chalcogenides to metal centers increases as  $\text{R}_3\text{PO} < \text{R}_3\text{PS} < \text{R}_3\text{PSe} < \text{R}_3\text{PTe}$ .<sup>84</sup> Infrared absorption spectroscopy and single crystal X-ray structural data show that tertiary phosphine chalcogenides coordinate Lewis acids through the chalcogen atom in either a unidentate fashion or by bridging two metal centers. Binding has also been studied with NMR and infrared spectroscopies. In the case of phosphine selenide and telluride, their coordination to a metal causes a decrease in the  $\text{P}-\text{E}$  coupling constant and a downfield shift in the  $^{31}\text{P}$  NMR peak of the phosphine chalcogenide.<sup>34</sup> Tertiary phosphine chalcogenide coordination to a metal weakens the  $\text{P}-\text{E}$  bond. For example, when triphenylphosphine selenide ( $\text{Ph}_3\text{PSe}$ ;  $d(\text{P}-\text{Se}) = 210.6$  pm) coordinates  $\text{HgCl}_2$  in  $\text{Ph}_3\text{PSeHgCl}_2$  ( $d(\text{P}-\text{Se}) = 217$  pm) the  $\text{PSe}$  bond length extends half way to the  $\text{P}-\text{Se}$  single bond distance ( $d(\text{P}-\text{Se}) = 224\text{--}228$  pm).<sup>84</sup> Coordination promotes

**Scheme 8. Equilibrium between Phosphine Tellurides, Phosphine, and Elemental Tellurium**



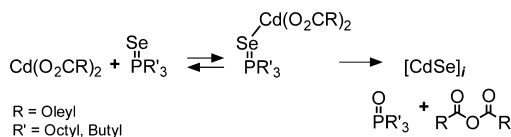


P–E cleavage and can lead to a complete bond cleavage to form a tertiary phosphine and chalcogenide atom that is incorporated in the metal complex.<sup>97,98</sup>

**P=E Cleavage Mechanisms.** Chalcogens are cleaved from phosphine chalcogenides by two pathways: (1) an acid/base mechanism in which the chalcogen transfers as E<sup>2−</sup> and (2) a redox mechanism where it transfers as E<sup>0</sup>. Both mechanisms are known to be important in ME nanocrystal synthesis depending on the reaction conditions.<sup>99,100</sup>

**Acid/Base (E<sup>2−</sup> transfer).** In this mechanism, R<sub>3</sub>PE undergoes nucleophilic attack, generally by an oxygen nucleophile, leading to cleavage of E<sup>2−</sup> with the production of a phosphine oxide coproduct. Steckel et al. proposed this mechanism to explain the coproducts formed from the reaction of TOPSe with lead oleate at 170 °C, which included PbSe, TOPO, and oleic anhydride.<sup>100</sup> Liu and co-workers reached a similar conclusion in their study of CdSe nanocrystal formation. By monitoring the reaction between metal phosphonate or carboxylate complexes and R<sub>3</sub>PE (M = Zn, Cd; R = *n*-octyl, *n*-butyl, *i*-propyl; E = S, Se, Te) they concluded that Lewis acid activation of the phosphine chalcogenide precedes the P–E cleavage step, leading to the pre-equilibrium Lewis acid activation mechanism shown in Scheme 9.<sup>34</sup> The conversion

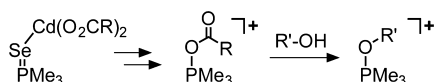
**Scheme 9. Chalcogenide Release Initiated by Nucleophilic Attack of Carboxylate on an Activated Phosphine Selenide**



rate was observed to increase in the order S < Se < Te and was sensitive to the steric properties of the phosphine with tri-*iso*-propylphosphine selenide undergoing much slower reaction than tri-*n*-butylphosphine selenide. The observed steric influence was later confirmed by monitoring the relative conversion rates of mixed aryl- and alkylphosphine selenides (Ph<sub>2</sub>BuP=Se < PhBu<sub>2</sub>P=Se < Octyl<sub>3</sub>P=Se).<sup>20</sup> A separate study concluded, however, that the P=E bond strength, rather than sterics, is a better predictor of reactivity.<sup>28</sup>

Garcia-Rodriguez et al. demonstrated that nucleophilic attack of carboxylate on trimethylphosphine selenide bound to cadmium carboxylate leads to an acyloxytrialkylphosphonium intermediate providing additional support for the earlier proposals (Scheme 10).<sup>101</sup> In their study, the acyloxytrialkylphosphonium ion was trapped in situ by reacting with an alcohol.

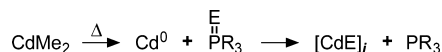
**Scheme 10. Formation and Trapping of an Acyloxyphosphonium Intermediate after P–Se Cleavage**



**Redox (E<sup>0</sup> Transfer).** Tri-*n*-alkylphosphine chalcogenides are well-known to oxidize transition and main group metals to the corresponding metal chalcogenide. This synthetic approach was developed by Steigerwald et al. and used to prepare a wide variety of materials, including clusters, nanocrystals and bulk materials.<sup>102–104</sup> These studies eventually led to the adoption of phosphine selenides in nanocrystal synthesis.

In nanocrystal syntheses, the production of M<sup>0</sup> often occurs by thermal decomposition of the starting metal complex or by chemical reduction. Thermal decomposition of CdMe<sub>2</sub> to Cd<sup>0</sup> occurs rapidly above 300 °C and has been used to synthesize Cd<sup>0</sup> nanocrystals that could be subsequently converted to CdE nanocrystals upon oxidation with R<sub>3</sub>PE (E = S, Se, Te) (Scheme 11).<sup>105,106</sup> Thermal decomposition of CdMe<sub>2</sub> can

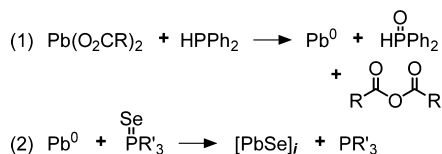
**Scheme 11. Thermal Decomposition of CdMe<sub>2</sub> and Its Oxidation by R<sub>3</sub>PE (E = S, Se)**



occur in parallel to its protonolysis with acidic surfactants, leading to syntheses with a net conversion rate that depends sensitively on the concentration of acidic surfactants and the injection step. This parallel path is thus likely to cause irreproducibility in syntheses that utilize a rapid injection of CdMe<sub>2</sub> at high temperature.<sup>20</sup>

A number of studies have concluded that lead carboxylates undergo reduction to Pb<sup>0</sup> en route to PbE nanocrystals, particularly in the presence of secondary phosphines. Steckel et al. was first to report that diphenylphosphine can reduce lead oleate to Pb<sup>0</sup> and diphenylphosphine oxide at >180 °C leading to PbSe nanocrystals (Scheme 12).<sup>100</sup> Later Joo et al. utilized

**Scheme 12. Proposed Reduction of Lead Carboxylate in the Synthesis of Lead Selenide**



diphenylphosphine and 1,2-hexadecanediol to reduce lead oleate to Pb<sup>0</sup>, which caused a significant increase in the yield of PbSe nanocrystals, albeit with a lower quantum yield.<sup>107</sup>

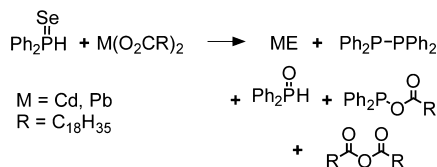
Evans et al. showed that at lower temperatures (120 °C) carefully purified Et<sub>3</sub>P=Se, *i*-Pr<sub>3</sub>P=Se, and Ph<sub>3</sub>P=Se are unreactive toward Pb(oleate)<sub>2</sub>, whereas addition of *i*-Pr<sub>2</sub>PH to these mixtures rapidly produced PbSe nanocrystals.<sup>108</sup> The authors conclude that exchange of chalcogen between tertiary and secondary phosphine chalcogenides leads to reaction rates that are entirely determined by the concentration of secondary phosphine. Furthermore, they propose lead diphenylphosphide intermediates to explain the observed coproducts and argue that Pb<sup>0</sup> formation and oxidation is too slow to account for the observed reaction rate.

Using <sup>31</sup>P NMR spectroscopy, Yu et al. found no evidence that TOPSe transferred selenium to Ph<sub>2</sub>PH despite a significant reduction in temperature at which ZnSe was observed to nucleate (260 °C vs 160 °C).<sup>109</sup> Thus, they suggested that Ph<sub>2</sub>PH increases the reactivity of the zinc ion rather than the chalcogenide. These authors drew a similar conclusion in their study of PbSe formation at low temperature (25–80 °C).<sup>110</sup> Furthermore, multiple studies have highlighted the presence of secondary phosphine impurities in commercially purchased tertiary phosphine,<sup>107,108</sup> and that these impurities increase its reactivity.<sup>109,110</sup> Similarly, the dioctylphosphine oxide found in commercial TOPO can disproportionate to dioctylphosphine and dioctylphosphinic acid, a reaction that increases the rate of precursor conversion.<sup>27</sup>

**Part IIIB: Secondary Phosphine Chalcogenides.** Secondary phosphine chalcogenides have also proven useful for nanocrystal synthesis.<sup>55,56,108,109</sup> Secondary phosphines react with elemental chalcogens to form the phosphine chalcogenide ( $R_2HP=E$ ) as well as dichalcogenido phosphinic acids ( $R_2P(E)EH$ ).<sup>86</sup> Both forms are generally synthesized by stirring a secondary phosphine ( $R_2PH$ ) with a stoichiometric amount of elemental chalcogen; overoxidation to the  $R_2P(E)EH$  form is a concern when the  $R_2HP=E$  species is desired. Secondary phosphine alkali metal chalcogenides can also be formed from the reaction of alkali-metal phosphides ( $M^+R_2P^-$ ) and the desired chalcogen.<sup>86</sup> Secondary phosphine chalcogenides bind to metals through the chalcogen atom, phosphorus atom, or both, leading to a wide range of binding motifs.<sup>93,97,111</sup> Likewise, chalcogenido phosphinate anions ( $R_2P(E)E^-$ ) bind metals in a bidentate fashion or by bridging two metal centers leading to dimers or polymers.<sup>86</sup>

The reaction of  $Ph_2HP=Se$  with metal carboxylates ( $M = Pb, Cd, Zn$ ) produces a variety of reaction coproducts depending on the reaction conditions, including  $Ph_2HP=O$ , tetraphenyldiphosphine ( $Ph_2PPPh_2$ ), carboxylic anhydride ( $RC(O)OC(O)R$ ), and diphenylphosphinocarboxylate  $Ph_2POC(O)R$  (Scheme 13).<sup>55,56,108</sup> At high concentrations of

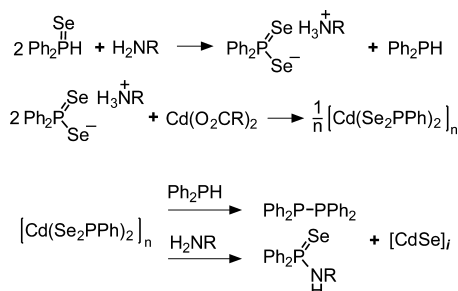
**Scheme 13. Reaction of Secondary Phosphine Selenide with Metal Carboxylate**



$Ph_2HPSe$  a lead diselenodiphenylphosphinate complex ( $Pb(Se_2PPh_2)_2$ ) was isolated and characterized by single crystal X-ray diffraction.<sup>108</sup> Cossairt and Owen studied the reaction of  $Ph_2HP=Se$  with cadmium benzoates in the presence of primary amines (45–115 °C) and observed that  $Ph_2HP=Se$  rapidly converts to  $[Ph_2PSe_2]^- [RNH_3]^+$  and  $Ph_2PH$ . Reaction with cadmium benzoate led to a cadmium dichalcogenido-phosphinate intermediate that subsequently converted to tetraphenyldiphosphine ( $Ph_2PPPh_2$ ) and selenophosphonamide ( $Ph_2P(Se)N(H)R$ ) coproducts (Scheme 14).<sup>55</sup>

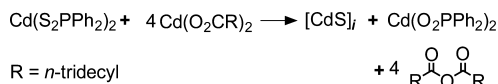
Hendricks et al. investigated the reaction of cadmium bis-diphenyldithiophosphinate ( $Cd(S_2PPh_2)_2$ ) with cadmium carboxylate en route to cadmium sulfide nanocrystals.<sup>56</sup> Much like earlier observations for the similar lead selenide complex,<sup>108</sup>  $Cd(S_2PPh_2)_2$  did not convert to CdS nanocrystals.

**Scheme 14. Conversion of Secondary Phosphine Selenide to CdSe in the Presence of Primary Amines**



However, when activated by at least four equivalents of cadmium tetradecanoate, CdS nanocrystals with narrow dispersity were produced in quantitative yield. Cadmium bis-diphenylphosphinate ( $Cd(O_2PPh_2)_2$ ) and tetradecanoic anhydride were produced as reaction coproducts, analogous to those identified upon conversion of tertiary phosphine chalcogenides under related conditions (Scheme 15). On the basis of the slow

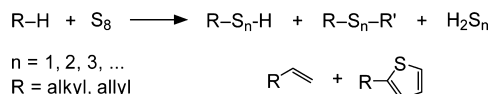
**Scheme 15. Reaction of Cadmium Dithiophosphinate with Cadmium Carboxylate To Generate CdS Nanocrystals**



reactivity in the absence of cadmium carboxylate and the reaction coproducts, the authors proposed a Lewis acid activation mechanism analogous to that suggested for tertiary phosphines.

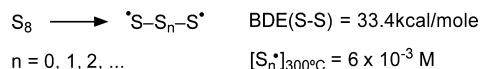
**Part IIIC: Sulfur and Selenium Dissolved in Octadecene and Amines.** *Reduction of Elemental Sulfur in Octadecene.* The reaction between elemental sulfur and hydrocarbons has long been studied for its relevance to the vulcanization of polyisoprene rubber. This reaction proceeds by a series of steps involving radical dehydrogenation, thiol–ene addition/elimination reactions, and polysulfide homologation, reactions leading to oligo-hydrosulfide, oligo-sulfide, and thiophene products (Scheme 16).<sup>112</sup> In particular, the reaction between paraffins and sulfur provides a convenient preparation of gaseous hydrogen sulfide<sup>113</sup> and has been used as an industrial source of thiophenes.<sup>114</sup>

**Scheme 16. Activation of Sulfur by Alkanes**



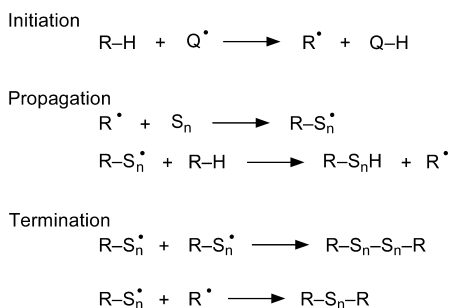
Radical dehydrogenation is driven in part by the ready homolysis of the S–S bond in  $S_8$  ( $BDE = 33.4 \text{ kcal/mol}$ ), which leads to millimolar concentrations of sulfur radicals in molten sulfur at 300 °C (Scheme 17).<sup>112,115</sup>

**Scheme 17. Sulfur Bond Homolysis**



Radical chain initiation and propagation proceeds via H-atom abstraction from the hydrocarbon substrate, leading to reaction rates that depend on its C–H bond strength (Scheme 18).<sup>112,116</sup> As a result, the stronger C–H bonds in alkanes ( $BDE(2^\circ \text{ C-H, propane}) = 95 \text{ kcal/mol}$ ) undergo more sluggish reaction than allylic C–H substrates ( $BDE(\text{allylic, propylene}) = 88 \text{ kcal/mol}$ ). Reaction rates are also known to be accelerated by Lewis acidic metals that absorb hydrogen sulfide, including zinc oxide and zinc propionate.<sup>117</sup>

1-Octadecene (ODE) and elemental sulfur were first used to make  $CdS^{31}$  and  $ZnS^{118}$  nanocrystals by injecting a mixture of sulfur dissolved in octadecene into a solution of cadmium oleate. Many syntheses use this approach, including preparations of  $Zn_xCd_{1-x}S$  nanocrystals.<sup>119,120</sup> Under these conditions, the hydrogen sulfide produced from the reaction between sulfur

**Scheme 18. Radical Chain Pathways in the Oxidation of Hydrocarbons by Elemental Sulfur**


and octadecene is proposed to lead to CdS as well as a carboxylic acid coproduct. In support of this hypothesis, Yordanov showed that the heating of elemental sulfur in various organic solvents yielded H<sub>2</sub>S, which formed CdS nanocrystals upon addition to cadmium carboxylate solution (Scheme 19).<sup>121</sup> In a study of sulfur dissolved in octadecene published

**Scheme 19. Reaction of H<sub>2</sub>S with Cadmium Carboxylate**


by Peng et al., tetradecylthiophene was detected by <sup>1</sup>H NMR spectroscopy and GC-MS in addition to carboxylic acid and carboxylic anhydride coproducts.<sup>122</sup>

In this system the rate of hydrogen sulfide production appears to limit the rate of CdS formation with the reaction rate becoming significant above 170 °C.<sup>122</sup> Consistent with previous studies on the radical dehydrogenation of hydrocarbons with sulfur, reactions conducted in octadecene solvent were more rapid than those run in alkane solution. Analogously, the synthesis of ZnS nanocrystals gave better results when conducted at higher temperatures (injection/growth = 340 °C/300 °C) compared with CdS nanocrystals (300 °C/250 °C), which was accomplished by using a mixture of tetracosane and octadecene.

One-pot syntheses of CdS nanocrystals from cadmium oleate, elemental sulfur, and octadecene have also been reported.<sup>123,124</sup> Under these conditions, radical chain initiators were introduced (tetraethylthiuram disulfide and 2,2-dithiobis-benzothiazole) that are known to accelerate rubber vulcanization.<sup>125</sup> Tuning the amount of the radical initiator provided a straightforward way to control particle size, with higher initiator concentrations leading to fewer numbers of nanocrystals and larger sizes. One-pot syntheses of CdS from 180 °C to greater than 220 °C have also been developed that do not require radical initiators.<sup>123,124,126</sup> In one case, sulfur dissolved in octadecene produces cadmium sulfide nanocrystals at faster rates than tri-*n*-butylphosphine sulfide. Using this difference in reactivity a core/shell nanocrystal Cd<sub>1-x</sub>Zn<sub>x</sub>S/ZnS could be synthesized.<sup>120</sup>

**Reduction of Elemental Selenium in Octadecene.** Despite the widespread use of sulfur dissolved in ODE, the synthesis of CdSe based on elemental selenium dissolved in ODE (Se-ODE) as a selenium source was not developed until 2005.<sup>80,126</sup> Since then it has been widely used as a convenient source of selenium for the formation of CdSe<sup>127</sup> and ZnSe nanocrystals,<sup>128</sup> CdSe nanoplatelets,<sup>129,130</sup> and CdSe<sup>131,132</sup> magic sized clusters. One pot methods that heat a mixture of selenium powder, cadmium tetradecanoate, and ODE to 240 °C are slow

to react until temperatures near the melting point of selenium (221 °C).

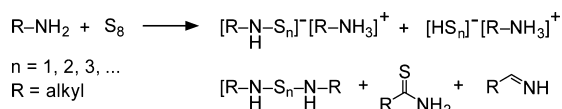
Heating of Se in hydrocarbon solvents (paraffin, *n*-hexadecane, ODE, TOPO, oleic acid, etc.) produces H<sub>2</sub>Se<sup>121,133,134</sup> via H-atom abstraction steps. Loss of hydrogen selenide to the headspace and the extent of the reaction influence the reactivity of these solutions, making this precursor's activity highly dependent on the method of preparation. Typically a transparent yellow solution is prepared by heating Se in ODE at 200 °C for 2 h. This solution is stable at room temperature under nitrogen; however, prolonged heating at 200 °C (more than 4 h) decreases its reactivity toward CdSe formation.<sup>80</sup> The active forms of selenium in this mixture are still under investigation. Although H<sub>2</sub>Se formed in situ is likely to form CdSe nanocrystals,<sup>134</sup> the structure of the organoselenium intermediates also appears important. Recent studies<sup>128,135</sup> suggest that slow deactivation of Se-ODE after prolonged heating results from slow degradation of Se-Se bonded intermediates in addition to gradual loss of H<sub>2</sub>Se. Several of these Se-Se and Se-C bonded species are visible using <sup>77</sup>Se NMR spectroscopy and X-ray absorption fine structure. Prolonged heating and deactivation is accompanied by a decrease in the number of Se-Se bonded species relative to the number of Se-C species suggesting that at this temperature not all intermediates are active for the production of CdSe.<sup>135</sup> <sup>1</sup>H NMR data also showed the terminal alkene of ODE (at 5.82 and 4.96 ppm) is converted to an internal olefin (5.41 ppm) indicating that allylic C-H oxidation may be followed by isomerization during the conversion reaction.<sup>135</sup>

Although the efficacy of Se-ODE depends on preparation temperature and time, Se-ODE is generally more reactive than TOPSe toward CdSe formation.<sup>135</sup> Mulvaney et al. utilized this difference by adding TOP to the ODE solution to tune its reactivity.<sup>80</sup> Increasing amounts of TOP leads to decreased number of nanocrystals, as well as an increase in the particle size.

**Tellurium.** A few reported attempts to use elemental tellurium and ODE in an analogous fashion for the synthesis of CdTe or ZnTe nanocrystals synthesis have failed, apparently due to its sluggish oxidation of the solvent.<sup>78,126</sup>

**Reduction of Sulfur and Selenium in Alkylamines.** The reaction of aliphatic amines with elemental sulfur produces a range of products arising from oxidation of the N-H and α-C-H bonds.<sup>112</sup> Many products have been identified including hydrosulfide, oligosulfide, and thioamide products, each of which can be further converted to additional equivalents of hydrogen sulfide by other decomposition routes. Among these reactions, nucleophilic cleavage of S-S bonds by the amine leads to ammonium oligo-sulfide salts, which have been isolated by crystallization.<sup>86,112,136</sup> Subsequent oxidation of the position α- to the amine terminus leads to other products shown in Scheme 20.

Despite the fact that reports on the chemistry of elemental sulfur "dissolved" in amines first appeared decades ago,<sup>86,112,136</sup> only recently have researchers paid attention to the implications

**Scheme 20. Reaction Products from the Oxidation of Alkylamines by Elemental Sulfur**




of this chemistry for the synthesis of nanocrystals. Ozin et al. investigated the role of octylammonium polysulfides,<sup>136–138</sup> formed in octylamine solution as precursors to metal sulfide nanocrystals.<sup>139</sup> The reaction byproducts, such as thioamides, were characterized by NMR analysis of the crude reaction. The authors suggest that the formation of thioamide is rate-limiting and that it should be considered as a potential sulfur precursor.<sup>139</sup>

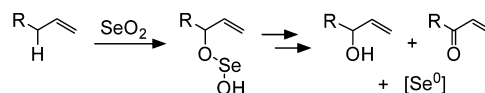
Hyeon has demonstrated the broad utility of elemental sulfur and several  $\text{MCl}_2$  salts ( $\text{M} = \text{Pb}, \text{Cd}, \text{Zn}, \text{Mn}$ ) dissolved in oleylamine (OLA). A combined injection and slow heating of the reaction mixture to a desired growth temperature 140–160 °C (CdS), 320 °C (ZnS), or 220 °C (PbS) can lead to large scale preparation of monodisperse nanocrystals.<sup>140</sup> Peng et al. demonstrated the utility of sulfur and octylamine for making cadmium sulfide nanocrystals at temperatures as low as 100 °C.<sup>122</sup>

In related chemistry, the use of sulfide salts (mostly  $\text{Na}_2\text{S}$ ) for the formation of metal chalcogenide nanocrystals has been explored predominantly in aqueous and biphasic solutions, and these reactions typically yield lower quality materials with high polydispersity as compared to organic phase reactions.<sup>141,142</sup> Notably, however, Robinson recently reported the scalable preparation of a variety of metal sulfide nanocrystals ( $\text{CdS}$ ,  $\text{Cu}_2\text{S}$ ,  $\text{SnS}$ ,  $\text{ZnS}$ ,  $\text{MnS}$ ,  $\text{Ag}_2\text{S}$ , and  $\text{Bi}_2\text{S}_3$ ) using the disulfide salt  $(\text{NH}_4)_2\text{S}_2$ , an  $\text{S}^{2-}$  source soluble in organic media.<sup>143</sup> The mechanism of this transformation is proposed to proceed through a straightforward salt elimination on mixing  $(\text{NH}_4)_2\text{S}$  with  $\text{MX}_2$ , generating the metal sulfide and  $(\text{NH}_4)\text{X}$ , with no involvement of the nanocrystal surfactants.<sup>143</sup>

**Part IIID:  $\text{SeO}_2$ .** Selenium dioxide ( $\text{SeO}_2$ ) is a white solid that sublimates at 317 °C at 70 mmHg and dissolves in water as selenous acid ( $\text{H}_2\text{SeO}_3$ ).<sup>144</sup> In the solid state,  $\text{SeO}_2$  has a polymeric structure made of pyramidal selenium atoms with three bound oxygen atoms ( $\text{SeO}_3$ ), one of which is terminal and the others bridging. In the gas phase it exists as monomeric  $\text{SeO}_2$ .<sup>145</sup> Recently Cao et al. reported a one pot synthesis of CdSe nanocrystals where  $\text{SeO}_2$  and cadmium tetradecanoate were heated to 240 °C in 1-octadecene.<sup>146</sup> Octadecene acts as both a solvent and reducing agent for the conversion of  $\text{SeO}_2$  to  $\text{Se}(0)$ , which presumably forms CdSe according to the pathways discussed above. Octadecane solvent also produced CdSe nanocrystals though in lower yield and with poor size distribution, while phenyl ether solvent was found to be comparatively unreactive. Hexadecanediol was also found to increase the number of nuclei providing a method to make smaller nanocrystals, though the mechanism of its effect is unknown. A similar strategy proved useful for making PbSe and PdSe nanocrystals, provided TOP and TOP/oleylamine were included. The method described by Cao was later adapted to prepare ZnSe nanocrystals using a stock solution of  $\text{SeO}_2$  in ODE which was prepared by dissolving  $\text{SeO}_2$  in ODE at 240 °C and was found to be stable for months.<sup>147</sup>

Selenium dioxide is a versatile oxidizing reagent in organic chemistry and is commonly used to convert allylic C–H bonds to the corresponding allylic alcohols or  $\alpha,\beta$ -unsaturated carbonyl compounds,<sup>148–151</sup> though a variety of organic molecules undergo dehydrogenation (Scheme 21).<sup>152,153</sup> The generally accepted mechanism of this allylic hydroxylation, proposed by Sharpless, starts with an electrophilic ene reaction followed by a [2,3] sigmatropic rearrangement leading to an intermediate seleninic acid.<sup>150</sup> Further conversion of this intermediate leads to alcohol and ketone products as well as

**Scheme 21. Activation of  $\text{SeO}_2$  by Unsaturated Hydrocarbons**



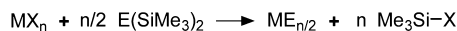
elemental selenium. At high temperature (300 °C)  $\text{SeO}_2$  dehydrogenates and decarboxylates long-chain saturated fatty acids ( $\text{C}_{12}$ – $\text{C}_{18}$ ) producing alkene byproducts<sup>152</sup> and oxidizes olefins to 1,2-dicarbonyl compounds.<sup>153</sup> Reduction of selenium dioxide to elemental selenium is driven by many reagents, including iodide and sulfide salts, as well as hydrazine and hydroxylamine.<sup>152</sup> These mechanisms likely operate in CdSe nanocrystal synthesis as well, where further reduction to hydrogen selenide occurs according to the mechanisms described above.

**Part IIIE: Silylchalcogenides.** Bis(trimethylsilyl) chalcogenides,  $(\text{Me}_3\text{Si})_2\text{E}$  ( $\text{E} = \text{S}, \text{Se}, \text{Te}$ ), are commonly used in organic chemistry as reducing agents<sup>154–156</sup> and as chalcogen atom transfer reagents.<sup>157–160</sup>  $(\text{Me}_3\text{Si})_2\text{E}$  has also been exploited for the preparation of II–VI complexes,<sup>161</sup> clusters,<sup>67,68,162,163</sup> and nanocrystals. Several trialkylsilyl chalcogenides are commercially available or readily prepared on multigram scales<sup>156,164–170</sup> by the reaction of  $\text{R}_3\text{SiCl}$  ( $\text{R} = \text{alkyl}$ ) and an alkali chalcogenide ( $\text{Na}_2\text{E}$  or  $\text{Li}_2\text{E}$ , typically prepared in situ) as was first reported by Abel.<sup>164</sup> The principal difference between the many synthetic routes that have since emerged is the way in which the in situ salt is prepared, though the reaction between  $\text{Li}_2\text{Se}$  and  $\text{R}_3\text{SiCl}$  can be slow unless excess selenium or  $\text{BF}_3$  etherate is present.<sup>169</sup>  $(\text{Me}_3\text{Si})_2\text{E}$  ( $\text{E} = \text{Se}, \text{Te}$ ) have been obtained by reducing  $\text{Se}$  or  $\text{Te}$  with  $\text{Na}$  or  $\text{Li}$  in liquid ammonia and subsequent reaction with  $\text{Me}_3\text{SiCl}$ .<sup>167,168</sup> Detty and Seidler employed  $\text{LiBHET}_3$  to reduce elemental chalcogen ( $\text{E} = \text{S}, \text{Se}, \text{Te}$ ), followed by the addition of  $\text{Me}_3\text{SiCl}$  in a one-pot process;<sup>156</sup> however, flammable coproducts are formed ( $\text{H}_2$  and  $\text{BEt}_3$ ) and these reaction mixtures should be handled with care.  $\text{Na}_2\text{S}$  has also been prepared from sodium in THF using sonication or naphthalene as a charge transfer agent.<sup>165</sup> Similarly,  $\text{Li}_2\text{Se}$  can be prepared from lithium and selenium in the presence of diphenylacetylene.<sup>169</sup> One notable exception avoiding the in situ synthesis of alkali metals was reported by Harpp and Steliou, who utilized hexamethyldisilazane and  $\text{H}_2\text{S}$  to prepare  $(\text{Me}_3\text{Si})_2\text{S}$ .<sup>166</sup>

Bis(trimethylsilyl) chalcogenides are air and moisture sensitive and decompose to the elemental chalcogen;<sup>163</sup> they should be stored under inert atmosphere and at low temperature. While  $(\text{Me}_3\text{Si})_2\text{S}$  is stable when stored in this manner,  $(\text{Me}_3\text{Si})_2\text{Se}$  gradually decomposes yielding elemental selenium and presumably  $(\text{Me}_3\text{Si})_2$  after about a month at –20 °C under argon,<sup>171</sup> and  $(\text{Me}_3\text{Si})_2\text{Te}$  is reported to decompose after 24 h, even when stored in the dark at –20 °C under argon.<sup>156</sup>  $(\text{Me}_2\text{tBuSi})_2\text{Te}$  is significantly more stable and is often used in place of  $(\text{Me}_3\text{Si})_2\text{Te}$ .<sup>156,172</sup>

$(\text{Me}_3\text{Si})_2\text{E}$  reagents react readily with many transition and main group metal salts (e.g., halides, acetates, metal alkyls), producing metal chalcogenide and the corresponding  $\text{Me}_3\text{Si-X}$  ( $\text{X} = \text{halogen, acetate, alkyl, usually } -\text{CH}_3$ ) as shown in Scheme 22.<sup>86,162,163</sup> The formation of the energetically favorable  $\text{Si-X}$  bond and the metal chalcogenide provide the driving force for this reaction.<sup>86,162</sup> Steigerwald investigated the reaction between  $\text{CdMe}_2$  and  $(\text{Me}_3\text{Si})_2\text{Se}$  at room temperature and showed the formation of CdSe and  $\text{SiMe}_4$ .<sup>71</sup> No other

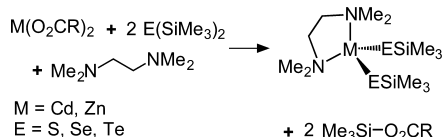


**Scheme 22. Reaction of Silylchalcogenides with Metal Salts**

X = halide, alkyl, carboxylate

species containing protons were observed during the reaction, arguing against a radical chain process. Interestingly, a strong dependence on the solvent was observed, where the reaction occurred instantaneously in dichloromethane, but was considerably slower in toluene. No reaction was observed if the reagents were combined without the use of a solvent.

Although trimethylsilyl chalcogen bonds are labile, especially in the case of the Se and Te derivatives,<sup>173,174</sup> several metal complexes have been reported with the fragment  $\text{Me}_3\text{SiE-M}$ . Bulky coligands were used to provide steric protection and to promote formation of monomeric complexes (Scheme 23).

**Scheme 23. Use of TMEDA as a Bulky Base To Generate Monomeric  $\text{ME}(\text{SiMe}_3)_2$  Species<sup>a</sup>**

<sup>a</sup>M = Zn, Cd.

The presence of an excess of a neutral ligand and at least equimolar amounts of  $(\text{Me}_3\text{Si})_2\text{E}$  with respect to the  $\text{AcO}^-$  groups on the metal were required to prevent subsequent reaction and avoid the generation of binary metal chalcogenides or polynuclear ME species.<sup>174–176</sup> These complexes containing a  $\text{Me}_3\text{SiE}$  ligand are unstable and decompose readily to polynuclear ME species even at low temperature.<sup>174,176</sup> The thermal stability of the Zn complexes with the  $\text{Me}_3\text{SiE}$  fragment shown in the Scheme 23 decreases in the order  $\text{S} > \text{Se} > \text{Te}$ .<sup>174</sup>

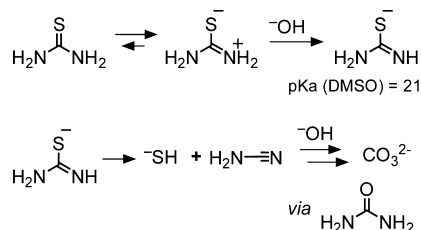
Early syntheses of CdSe nanocrystals utilized  $(\text{Me}_3\text{Si})_2\text{Se}$  and aqueous  $\text{Cd}^{2+}$  in Aerosol-OT/ $\text{H}_2\text{O}$ /heptane reverse-micelle solutions (Aerosol-OT: bis(2-ethylhexyl) sulfosuccinate).<sup>72</sup> Later cadmium chalcogenide nanocrystals were synthesized by injecting  $\text{CdMe}_2$  and  $(\text{R}_3\text{Si})_2\text{E}$  (E = S, Se) or  $(\text{Me}_2\text{tBuSi})_2\text{Te}$  into TOP/TOPO at approximately 100 °C, temperatures much lower than those required for efficient reaction with TOPSe or TOPTe.<sup>45</sup> Despite its early prominence in the development of CdE syntheses, the use of  $(\text{Me}_3\text{Si})_2\text{E}$  in the preparation of II–VI colloidal nanocrystals is relatively rare and is mainly limited to the synthesis of CdS nanocrystals.<sup>177</sup> Recently,  $(\text{Me}_3\text{Si})_2\text{S}$  has been employed in the synthesis of CdS magic-sized clusters via a one-pot noninjection approach.<sup>178</sup> In this method the high reactivity of  $(\text{Me}_3\text{Si})_2\text{S}$  allowed the synthesis to be performed at lower temperatures (~100 °C).

$(\text{Me}_3\text{Si})_2\text{E}$  is commonly used as a reagent for the growth of shells on various semiconductor nanocrystal cores. For example, reaction between  $\text{CdMe}_2$  or  $\text{ZnEt}_2$  and  $(\text{Me}_3\text{Si})_2\text{S}$  can be used to prepare highly luminescent CdSe/CdS or CdSe/ZnS core/shell nanocrystals.<sup>179,180</sup> This has been subsequently modified to grow other CdSe/ZnS core/shell nanocrystals,<sup>50,181,182</sup> as well as to prepare the final ZnS layer of a ZnS/CdSe/ZnS quantum-well structure.<sup>183</sup>  $(\text{Me}_3\text{Si})_2\text{Se}$  has also been employed to grow CdSe on a ZnS nanocrystal.<sup>184</sup>

In contrast to the literature on II–VI nanocrystals,  $(\text{Me}_3\text{Si})_2\text{S}$  is often used to synthesize of PbS nanocrystals.<sup>185–188</sup> A recent report, utilizing a mixture of two chalcogenide precursors,

compared relative incorporation of S, Se, or Te into the resultant alloyed nanocrystals ( $\text{PbS}_x\text{Te}_{1-x}$ ,  $\text{PbS}_x\text{Se}_{1-x}$ , and  $\text{PbSe}_x\text{Te}_{1-x}$ ).<sup>189</sup> On the basis of ICP-AES data the authors concluded that trimethylsilylchalcogenides are more reactive than tri-*n*-alkylphosphine chalcogenides. They also measured a preference for the incorporation of tellurium over sulfur and sulfur over selenium. The latter trend differs from the cleavage rates of phosphine chalcogenides  $\text{S} < \text{Se} < \text{Te}$ <sup>34</sup> and also differs from previous studies on the stability of  $(\text{Me}_3\text{Si})_2\text{E}$ .<sup>174</sup>

**Part IIIF: Ureas.** Thiourea and selenourea are among the most common precursors used to prepare metal chalcogenide nanocrystals in aqueous solution. Hydrolysis of the C–Se bonds is accelerated under basic conditions allowing the hydrosulfide production rate to be tuned using the solution pH.<sup>190</sup> Thiourea is a relatively mild acid ( $\text{pK}_a(\text{DMSO}) = 21$ )<sup>191</sup> and ionizes in neutral water (no information regarding the second  $\text{pK}_a$  could be found). The anion then undergoes a subsequent reaction with base leading to a linear pH dependence of the hydrosulfide production rate (Scheme 24).<sup>192</sup> A variety of hydrolysis products are formed, depending

**Scheme 24. Decomposition of Thiourea in Basic Media<sup>192</sup>**

on the reaction conditions, including cyanamide, cyanate, urea, and carbonate.<sup>193,194</sup> The details of this mechanism are likely to change in the presence of thiophilic Lewis acidic metal ions like zinc and cadmium.

There are fewer reports on selenoureas, perhaps because of their sensitivity to light and air and their more involved synthesis.<sup>195</sup> Substituted thioureas and selenoureas can be prepared, in a general way, by the reaction of amines with isothiocyanate<sup>196–198</sup> or isoselenocyanate,<sup>199–203</sup> or by the reaction of carbodiimides<sup>204</sup> or cyanamides<sup>205</sup> with  $\text{LiAlHEH}$  (E = S, Se) or carbon disulfide.<sup>206,207</sup> There are few reports describing telloureas, most likely due their involved preparation and the labile nature of the  $\text{C}=\text{Te}$  bond,<sup>208</sup> which readily releases elemental tellurium.<sup>209</sup>

Among all urea derivatives, only thiourea and selenourea have been widely used in the synthesis of metal chalcogenide nanocrystals. Thiourea has been used to prepare a variety of cadmium sulfide nanocrystals including nanorods,<sup>210–212</sup> nanowires,<sup>213–215</sup> and CdS-Mn/ZnS core-shell nanowires,<sup>216</sup> as well as to grow CdS<sup>217</sup> shells. Similar methods employing thiourea have been adapted to prepare ZnS nanosheets,<sup>218</sup> ZnS nanorods,<sup>219,220</sup> and nanowires,<sup>221</sup> and to grow ZnS<sup>222,223</sup> shells. Ultrasonic irradiation has been used to induce decomposition of thiourea or selenourea in aqueous solution to prepare ZnS,<sup>224</sup> CdS,<sup>225–227</sup> and ZnSe.<sup>228</sup> Although less commonly employed, microwave irradiation has also been used to induce decomposition of thiourea and selenourea in the preparation of CdS,<sup>229,230</sup> CdSe,<sup>231</sup> and ZnSe<sup>231</sup> nanocrystals. Pan and co-workers developed a two-phase approach to prepare CdS<sup>232</sup> and CdSe<sup>233</sup> nanocrystals. The method was later modified by using an autoclave<sup>234–236</sup> and introducing

new chalcogenide sources to control the nucleation and growth rate. The reactivity trends found were  $\text{NaHS} > \text{selenourea} > \text{Na}_2\text{SeSO}_3$  and  $\text{Na}_2\text{S} > \text{thiourea}$ .<sup>235</sup>

ZnS nanocrystals have also been prepared using a low temperature colloidal method based on the injection of thiourea into a solution of tetramethylammonium hydroxide and  $\text{ZnCl}_2$  dissolved in ethylene glycol (100 °C).<sup>237</sup> Schaak and Dawood demonstrated that this reaction proceeded through the formation of wurtzite ZnO as an intermediate.<sup>238</sup> The reaction of selenourea with hydrates of  $\text{Cd}(\text{ClO}_4)_2$ <sup>239</sup> or  $\text{Cd}(\text{O}_2\text{CMe})_2$ <sup>240</sup> in pyridine at 80 °C also produces CdSe nanocrystals. Microwave irradiation has been used to prepare CdSe<sup>231</sup> and ZnSe<sup>231</sup> nanocrystals from selenourea in dimethylformamide.<sup>229,230</sup>

A variety of studies used thiourea and selenourea to prepare II–VI nanostructures in dry organic media, although the conversion mechanism is unclear. For example, ultrathin ZnSe nanorods and nanowires formed by reaction of selenourea with  $\text{Zn}(\text{O}_2\text{CMe})_2$  in octadecylamine,<sup>241</sup> ZnSe nanocrystals,<sup>242</sup> and spherical ZnSe nanocrystals<sup>243</sup> have all been reported. Similarly, Peng et al. obtained ultrathin CdSe nanowires by reacting cadmium acetate and selenourea in long-chain amines at low temperature (100–180 °C).<sup>244</sup> Recently, Buhro et al. used cadmium acetate and selenourea in octylamine to prepare CdSe quantum belts<sup>79,245</sup> by a modification of the procedure of Peng.<sup>244</sup> While hydrolysis of the urea is a possibility, elimination of elemental selenium may also lead to amine oxidation by the pathways described above. Related compounds such as thioacetamide<sup>246,247</sup> or selenocarbamates<sup>248</sup> have been used as well.

**Part IIIG: Additional Telluride Sources.** Tellurium precursors for the preparation of II–VI colloidal nanocrystals have been explored less than have precursors for the other chalcogens. In this regard, it is worth mentioning some characteristics of tellurium. In contrast with sulfur and selenium, which are present in a variety of allotropes, tellurium has only a single crystalline form composed of helical chains. Tellurium hydride is also the least stable hydride, with the thermal stability of the hydrides following the trend  $\text{H}_2\text{O} > \text{H}_2\text{S} > \text{H}_2\text{Se} > \text{H}_2\text{Te}$ .<sup>144</sup> Tellurium is less easily reduced to  $\text{Te}^{2-}$  compared with selenium and sulfur as can be observed by comparing the standard reduction potentials of Se and Te in aqueous solution:  $\text{Te}(\text{s}) + 2\text{e}^- \rightarrow \text{Te}^{2-}$ ,  $E^\circ = -1.14$ ;  $\text{Se}(\text{s}) + 2\text{e}^- \rightarrow \text{Se}^{2-}$ ,  $E^\circ = -0.92$  V (V vs SHE at 25 °C).<sup>249</sup> Nevertheless, much like elemental selenium, elemental tellurium undergoes reduction to  $\text{Te}^{2-}$  by superhydride ( $\text{LiBHET}_3$ ) in tetrahydrofuran and  $\text{NaBH}_4$  in ethanol solution.<sup>250</sup> Much like polysulfides and polyselenides, oligomeric telluride anions,  $\text{Te}_x^{2-}$ , are known for  $x = 2-5, 8, 12$ , and  $13$ .<sup>251</sup>

The synthesis of colloidal MTe nanocrystals ( $M = \text{Zn}, \text{Cd}, \text{Hg}, \text{Pb}$ ) is less well-developed compared with their selenide and sulfide counterparts. Among these, the synthesis of CdTe nanocrystals in aqueous solution has been explored most extensively and is the subject of a recent review.<sup>252</sup> These methods utilize aqueous solutions of  $\text{Na}_2\text{Te}$ ,<sup>253</sup>  $\text{H}_2\text{Te}$ ,<sup>254</sup> and  $\text{NaHTe}$ ,<sup>255,256</sup> prepared from Te and  $\text{NaBH}_4$ , to synthesize CdTe in the presence of sulfur-containing ligands, such as thioglycerol, thioglycolic acid, mercaptopropionic acid, and mercaptoethanol. In organic solution the reaction of tertiary alkylphosphine tellurides is the most common approach, though it has been described by only a few reports (see Section IIIA). A recent report describes a combination of  $\text{R}_3\text{P} = \text{Te}$  and  $[\text{Li}]^+[\text{Et}_3\text{BH}]^-$  that produces oligotelluride anions

( $\text{Te}_n^{2-}$ ,  $n = 1, 2, 3$ ), the speciation of which depends on the amount of hydride reducing agent.<sup>257</sup> Oligotellurides lead to slower ZnTe production and anisotropic shapes while  $\text{Te}^{2-}$  was found to be most reactive and lead to small ( $d = 3.5$  nm), spherical ZnTe nanocrystals.

The inability to adapt traditional sulfur and selenium precursors for the corresponding tellurium species seems to arise from the weakness of  $\text{Te}-\text{C}$ ,  $\text{Te}-\text{Si}$ , and  $\text{Te}=\text{P}$  bonds, yielding very reactive or unstable compounds. For instance, no telluroreas have been developed as tellurium precursors, and  $(\text{R}_3\text{Si})_2\text{Te}$  is unstable unless the alkylsilyl groups are sterically bulky  $(\text{Me}_2^t\text{BuSi})_2\text{Te}$ .<sup>78,258</sup> In the search for greener methods that avoid the use of phosphines in nanocrystal synthesis, methods based on the use of elemental sulfur and selenium dissolved in amines and/or octadecene have been developed (see Section IIIC). Unfortunately, little progress has been made in the development of an analogous tellurium-based method.<sup>78</sup> Elemental tellurium is unreactive toward octadecene, perhaps because its melting point is quite high ( $\text{m.p.}(\text{Te}) = 452$  °C  $>$   $\text{m.p.}(\text{Se}) = 217.5$  °C  $>$   $\text{m.p.}(\text{S}) = 119$  °C).<sup>144</sup>

Recently CdTe and PbTe nanocrystals were prepared by heating a mixture of  $\text{TeO}_2$  and TOPO (90% purity) at 380 °C, followed by injection of the metal carboxylate to the reaction solution.<sup>259</sup> The identity of the active tellurium species is unknown in these transformations; however, it was shown that TOPO reduces  $\text{TeO}_2$  producing octyl-di-*n*-octylphosphinate and elemental Te.<sup>259</sup> Recently, elemental tellurium was shown to dissolve in 90% TOPO at 400 °C to form a stable yellow solution which was later used to produce CdTe nanocrystals.<sup>85</sup>

## ■ CONCLUSIONS AND PERSPECTIVES: THE IMPORTANCE OF PRECURSOR CHEMISTRY

The synthesis of colloidal semiconductor nanocrystals has been under investigation for nearly 30 years. A high degree of size and shape control has been achieved with selected material–shape combinations (e.g., CdSe dots and rods). While in some cases scalable and reproducible reactions have been achieved and conditions can be chosen to obtain a particular structure, much work is needed to establish the mechanisms of reactions and to use this information to improve the outcome. Indeed, the fabrication of inorganic nanostructures is still at its infancy. More detailed investigations of precursor reactivity and coproducts are needed to conduct reactions that provide high yields of a desired structure on large scales. This challenge will become more pressing as nanocrystal technologies transition to market, as researchers develop multistep transformations for the synthesis of nanocrystal heterostructures, and as they seek to understand the composition of the nanocrystal products. Despite this, only a few precursor reactions mechanisms have been proposed and investigated, and there are clear opportunities for future learning in this regard.

## ■ AUTHOR INFORMATION

### Corresponding Author

\*E-mail: cossairt@chem.washington.edu (B.M.C.); hliu@pitt.edu (H.L.); jso2115@columbia.edu (J.S.O.).

### Author Contributions

||R.G.-R. and M.P.H. contributed equally to the preparation of this review.

### Notes

The authors declare no competing financial interest.

## ACKNOWLEDGMENTS

R.G.-R. acknowledges Fundación Ramón Areces for a postdoctoral fellowship. J.S.O. acknowledges financial support from Columbia University and the National Science Foundation through Contract No. NSF-CHE-1151172 during the preparation of this manuscript. B.M.C. acknowledges support from University of Washington during the preparation of this manuscript.

## REFERENCES

- (1) Schaak, R. E.; Williams, M. E. *ACS Nano* **2012**, *6*, 8492–8497.
- (2) Watzky, M. A.; Finke, R. G. *J. Am. Chem. Soc.* **1997**, *119*, 10382–10400.
- (3) Shields, S. P.; Richards, V. N.; Buhro, W. E. *Chem. Mater.* **2010**, *22*, 3212–3225.
- (4) Richards, V. N.; Rath, N. P.; Buhro, W. E. *Chem. Mater.* **2010**, *22*, 3556–3567.
- (5) Richards, V. N.; Shields, S. P.; Buhro, W. E. *Chem. Mater.* **2011**, *23*, 137–144.
- (6) Finney, E. E.; Shields, S. P.; Buhro, W. E.; Finke, R. G. *Chem. Mater.* **2012**, *24*, 1718–1725.
- (7) Yin, Y.; Alivisatos, A. P. *Nature* **2005**, *437*, 664–670.
- (8) Cozzoli, P. D.; Pellegrino, T.; Manna, L. *Chem. Soc. Rev.* **2006**, *35*, 1195–1208.
- (9) Park, J.; Joo, J.; Kwon, S. G.; Jang, Y.; Hyeon, T. *Angew. Chem., Int. Ed.* **2007**, *46*, 4630–4660.
- (10) Finney, E. E.; Finke, R. G. *J. Colloid Interface Sci.* **2008**, *317*, 351–374.
- (11) Zhang, J.; Huang, F.; Lin, Z. *Nanoscale* **2010**, *2*, 18–34.
- (12) Zhuang, Z. B.; Peng, Q.; Li, Y. D. *Chem. Soc. Rev.* **2011**, *40*, 5492–5513.
- (13) Exceptions to this scheme include autocatalytic conversion reactions that occur at the surface of metal nanocrystals (see ref 10), and indirect mechanisms like a change in the viscosity of the reaction medium etc.
- (14) Lamer, V. K.; Dinegar, R. H. *J. Am. Chem. Soc.* **1950**, *72*, 4847–4854.
- (15) Sugimoto, T. *Monodispersed particles*; Elsevier Science: Amsterdam, 2001.
- (16) Sugimoto, T.; Shiba, F.; Sekiguchi, T.; Itoh, H. *Colloids Surf., A* **2000**, *164*, 183–203.
- (17) Sugimoto, T. *J. Colloid Interface Sci.* **2007**, *309*, 106–118.
- (18) Rempel, J. Y.; Bawendi, M. G.; Jensen, K. F. *J. Am. Chem. Soc.* **2009**, *131*, 4479–4489.
- (19) Abe, S.; Capek, R. K.; De Geyter, B.; Hens, Z. *ACS Nano* **2012**, *6*, 42–53.
- (20) Owen, J. S.; Chan, E. M.; Liu, H. T.; Alivisatos, A. P. *J. Am. Chem. Soc.* **2010**, *132*, 18206–18213.
- (21) Yordanov, G. G.; Dushkin, C. D.; Adachi, E. *Colloids Surf., A* **2008**, *316*, 37–45.
- (22) Yordanov, G. G.; Yoshimura, H.; Dushkin, C. D. *Colloids Surf., A* **2008**, *322*, 177–182.
- (23) Chan, E. M.; Xu, C.; Mao, A. W.; Han, G.; Owen, J. S.; Cohen, B. E.; Milliron, D. J. *Nano Lett.* **2010**, *10*, 1874–1885.
- (24) Sugimoto, T. *Adv. Colloid Interface Sci.* **1987**, *28*, 65–108.
- (25) Clark, M. D.; Kumar, S. K.; Owen, J. S.; Chan, E. M. *Nano Lett.* **2011**, *11*, 1976–1980.
- (26) Peng, Z. A.; Peng, X. *J. Am. Chem. Soc.* **2002**, *124*, 3343–3353.
- (27) Wang, F. D.; Buhro, W. E. *J. Am. Chem. Soc.* **2012**, *134*, 5369–5380.
- (28) Ruberu, T. P. A.; Albright, H. R.; Callis, B.; Ward, B.; Cisneros, J.; Fan, H. J.; Vela, J. *ACS Nano* **2012**, *6*, 5348–5359.
- (29) Bullen, C. R.; Mulvaney, P. *Nano Lett.* **2004**, *4*, 2303–2307.
- (30) van Embden, J.; Mulvaney, P. *Langmuir* **2005**, *21*, 10226–10233.
- (31) Yu, W. W.; Peng, X. *Angew. Chem., Int. Ed.* **2002**, *41*, 2368–2371.
- (32) Mehrotra, R. C.; Bohra, R. *Metal Carboxylates*; Academic Press: London, 1983.
- (33) Pilpel, N. *Chem. Rev.* **1963**, *63*, 221–234.
- (34) Liu, H.; Owen, J. S.; Alivisatos, A. P. *J. Am. Chem. Soc.* **2007**, *129*, 305–312.
- (35) Houtepen, A. J.; Koole, R.; Vanmaekelbergh, D. V.; Meeldijk, J.; Hickey, S. G. *J. Am. Chem. Soc.* **2006**, *128*, 6792–6793.
- (36) Zhu, M.; Lanni, E.; Garg, N.; Bier, M. E.; Jin, R. *J. Am. Chem. Soc.* **2008**, *130*, 1138–1139.
- (37) Mesubi, M. A. *J. Mol. Struct.* **1982**, *81*, 61–71.
- (38) Deacon, G. B.; Phillips, R. J. *Coord. Chem. Rev.* **1980**, *33*, 227–250.
- (39) Stamatatos, T.; Katsoulakou, E.; Nastopoulos, V.; Raptopoulou, C.; Manessi-Zoupa, E.; Perlepes, S. Z. *Nat. B* **2003**, *58*, 1045–1054.
- (40) Akanni, M. S.; Okoh, E. K.; Burrows, H. D.; Ellis, H. A. *Thermochim. Acta* **1992**, *208*, 1–41.
- (41) Malecka, B.; Lacz, A. *Thermochim. Acta* **2008**, *479*, 12–16.
- (42) Qu, L.; Peng, Z.; Peng, X. *Nano Lett.* **2001**, *1*, 333–337.
- (43) Zhong, X.; Feng, Y.; Zhang, Y. J. *J. Phys. Chem. C* **2007**, *111*, 526–531.
- (44) Bania, K.; Barooah, N.; Baruah, J. B. *Polyhedron* **2007**, *26*, 2612–2620.
- (45) Murray, C. B.; Norris, D. J.; Bawendi, M. G. *J. Am. Chem. Soc.* **1993**, *115*, 8706–8715.
- (46) Wang, F.; Tang, R.; Buhro, W. E. *Nano Lett.* **2008**, *8*, 3521–3524.
- (47) Peng, X.; Manna, L.; Yang, W.; Wickham, J.; Scher, E.; Kadavanich, A.; Alivisatos, A. *Nature* **2000**, *404*, 59–61.
- (48) Peng, Z. A.; Peng, X. *J. Am. Chem. Soc.* **2001**, *123*, 183–184.
- (49) Kopping, J. T.; Patten, T. E. *J. Am. Chem. Soc.* **2008**, *130*, 5689–5698.
- (50) Owen, J. S.; Park, J.; Trudeau, P.-E.; Alivisatos, A. P. *J. Am. Chem. Soc.* **2008**, *130*, 12279–12281.
- (51) Frederick, M.; Achtyl, J.; Knowles, K.; Weiss, E.; Geiger, F. J. *J. Am. Chem. Soc.* **2011**, *133*, 7476–7481.
- (52) Morris-Cohen, A.; Frederick, M.; Lilly, G.; McArthur, E.; Weiss, E. *J. Phys. Chem. Lett.* **2010**, *1*, 1078–1081.
- (53) Morris-Cohen, A.; Vasilenko, V.; Amin, V.; Reuter, M.; Weiss, E. *ACS Nano* **2012**, *6*, 557–565.
- (54) Wang, F.; Tang, R.; Kao, J. L. F.; Dingman, S. D.; Buhro, W. E. *J. Am. Chem. Soc.* **2009**, *131*, 4983–4994.
- (55) Cossairt, B. M.; Owen, J. S. *Chem. Mater.* **2011**, *23*, 3114–3119.
- (56) Hendricks, M. P.; Cossairt, B. M.; Owen, J. S. *ACS Nano* **2012**, *6*, 10054–10062.
- (57) *Metal phosphonate chemistry: From synthesis to applications*; Clearfield, A.; Demadis, K., Eds.; RSC Publishing: Cambridge, 2011.
- (58) Hambrock, J.; Birkner, A.; Fischer, R. *J. Mater. Chem.* **2001**, *11*, 3197–3201.
- (59) Chandrasekhar, V.; Sasikumar, P.; Boomishankar, R. *Dalton Trans.* **2008**, 5189–5196.
- (60) Cao, G.; Lynch, V. M.; Yacullo, L. N. *Chem. Mater.* **1993**, *5*, 1000–1006.
- (61) Anantharaman, G.; Walawalkar, M. G.; Murugavel, R.; Gábor, B.; Herbst-Imer, R.; Baldus, M.; Angerstein, B.; Roesky, H. W. *Angew. Chem., Int. Ed.* **2003**, *42*, 4482–4485.
- (62) Frink, K. J.; Wang, R. C.; Colon, J. L.; Clearfield, A. *Inorg. Chem.* **1991**, *30*, 1438–1441.
- (63) Bochmann, M.; Coleman, A. P.; Webb, K. J.; Hursthouse, M. B.; Mazid, M. *Angew. Chem., Int. Ed.* **1991**, *30*, 973–975.
- (64) Dance, I. G.; Garbutt, R. G.; Craig, D. C.; Scudder, M. L. *Inorg. Chem.* **1987**, *26*, 4057–4064.
- (65) Kedarnath, G.; Jain, V. K.; Wadawale, A.; Dey, G. K. *Dalton Trans.* **2009**, 8378–8385.
- (66) Anjali, K.; Vittal, J. *Inorg. Chem. Commun.* **2000**, *3*, 708–710.
- (67) Corrigan, J. F.; Fuhr, O.; Fenske, D. *Adv. Mater.* **2009**, *21*, 1867–1871.
- (68) Soloviev, V. N.; Eichhoefer, A.; Fenske, D.; Banin, U. *J. Am. Chem. Soc.* **2001**, *123*, 2354–2364.
- (69) Dance, I. G. *J. Am. Chem. Soc.* **1980**, *102*, 3445–3451.



- (70) Amberson, S. J.; Einstein, F. W. B.; Hayes, P. C.; Kumar, R.; Tuck, D. G. *Inorg. Chem.* **1986**, *25*, 4181–4184.
- (71) Stuczynski, S. M.; Brennan, J. G.; Steigerwald, M. L. *Inorg. Chem.* **1989**, *28*, 4431–4432.
- (72) Steigerwald, M. L.; Alivisatos, A. P.; Gibson, J. M.; Harris, T. D.; Kortan, R.; Muller, A. J.; Thayer, A. M.; Duncan, T. M.; Douglass, D. C.; Brus, L. E. *J. Am. Chem. Soc.* **1988**, *110*, 3046–3050.
- (73) Cumberland, S. L.; Hanif, K. M.; Javier, A.; Khitrov, G. A.; Strouse, G. F.; Woessner, S. M.; Yun, C. S. *Chem. Mater.* **2002**, *14*, 1576–1584.
- (74) Archer, P. I.; Santangelo, S. A.; Gamelin, D. R. *J. Am. Chem. Soc.* **2007**, *129*, 9808–9818.
- (75) Malik, M. A.; Afzaal, M.; O'Brien, P. *Chem. Rev.* **2010**, *110*, 4417–4446.
- (76) Ritch, J. S.; Chivers, T.; Afzaal, M.; O'Brien, P. *Chem. Soc. Rev.* **2007**, *36*, 1622–1631.
- (77) Manna, L.; Scher, E.; Alivisatos, A. J. *Cluster Sci.* **2002**, *13*, 521–532.
- (78) Son, J. S.; Wen, X.-D.; Joo, J.; Chae, J.; Baek, S.-i.; Park, K.; Kim, J. H.; An, K.; Yu, J. H.; Kwon, S. G.; Choi, S.-H.; Wang, Z.; Kim, Y.-W.; Kuk, Y.; Hoffmann, R.; Hyeon, T. *Angew. Chem., Int. Ed.* **2009**, *48*, 6861–6864.
- (79) Liu, Y.-H.; Wang, F.; Wang, Y.; Gibbons, P. C.; Buhro, W. E. *J. Am. Chem. Soc.* **2011**, *133*, 17005–17013.
- (80) Jasieniak, J.; Bullen, C.; Van, E. J.; Mulvaney, P. *J. Phys. Chem. B* **2005**, *109*, 20665–20668.
- (81) Zingaro, R.; McGlothlin, R. J. *Chem. Eng. Data* **1963**, *8*, 226–229.
- (82) Capps, K. B.; Wixmerten, B.; Bauer, A.; Hoff, C. D. *Inorg. Chem.* **1998**, *37*, 2861–2864.
- (83) Horner, L.; Winkler, H.; Rapp, A.; Mentrup, A.; Hoffmann, H.; Beck, P. *Tetrahedron Lett.* **1961**, *2*, 161–166.
- (84) Lobana, T. S. *Prog. Inorg. Chem.* **1989**, *37*, 495–581.
- (85) Xu, W.; Shen, H.; Niu, J. Z.; Zhou, C.; Yu, C.; Li, X.; Hang, Y.; Wang, H.; Ma, L.; Li, L. S. *CrystEngComm* **2012**, *14*, 272–277.
- (86) Devillanova, F. A., Ed. *Handbook of chalcogen chemistry: New perspectives in sulfur, selenium and tellurium*; Royal Society of Chemistry: 2007.
- (87) Jiang, Z.-J.; Kelley, D. F. *ACS Nano* **2010**, *4*, 1561–1572.
- (88) Zingaro, R. A.; Steeves, B. H.; Irgolic, K. J. *Organomet. Chem.* **1965**, *4*, 320–323.
- (89) Dean, P. A. W. *Can. J. Chem.* **1979**, *57*, 754–761.
- (90) Clive, D. L. J.; Beaulieu, P. L. *J. Org. Chem.* **1982**, *47*, 1124–1126.
- (91) Hartley, F. R. The chemistry of organophosphorus compounds. *Phosphine oxides, sulphides, selenides and tellurides*; John Wiley & Sons: Chichester, 1992; Vol. 2.
- (92) Davies, R. *Handbook of chalcogen chemistry: New perspectives in sulfur, selenium and tellurium*; The Royal Society of Chemistry: 2007; pp 286–343.
- (93) Davies, R.; Francis, C.; Jurd, A.; Martinelli, M.; White, A.; Williams, D. *Inorg. Chem.* **2004**, *43*, 4802–4804.
- (94) Baechler, R. D.; Stack, M.; Stevenson, K.; Vanvalkenburgh, V. *Phosphorus, Sulfur, Silicon Relat. Elem.* **1990**, *48*, 49–52.
- (95) Du Mont, W. W.; Kroth, H. J. *J. Organomet. Chem.* **1976**, *113*, C35–C37.
- (96) Brown, D. H.; Cross, R. J.; Millington, D. J. *Organomet. Chem.* **1977**, *125*, 219–223.
- (97) Walther, B. *Coord. Chem. Rev.* **1984**, *60*, 67–105.
- (98) Schilling, E. L. a. B. *Chem. Ber. Recl.* **1977**, *110*, 3725.
- (99) Steigerwald, M. L.; Brus, L. E. *Annu. Rev. Mater. Sci.* **1989**, *19*, 471–495.
- (100) Steckel, J. S.; Yen, B. K. H.; Oertel, D. C.; Bawendi, M. G. *J. Am. Chem. Soc.* **2006**, *128*, 13032–13033.
- (101) Garcia-Rodriguez, R.; Liu, H. J. *J. Am. Chem. Soc.* **2012**, *134*, 1400–1403.
- (102) Brennan, J. G.; Siegrist, T.; Stuczynski, S. M.; Steigerwald, M. L. *J. Am. Chem. Soc.* **1989**, *111*, 9241–9242.
- (103) Steigerwald, M. L.; Sprinkle, C. R. *Organometallics* **1988**, *7*, 245–246.
- (104) Steigerwald, M. L.; Rice, C. E. *J. Am. Chem. Soc.* **1988**, *110*, 4228–4231.
- (105) Ibanez, M.; Fan, J.; Li, W.; Cadavid, D.; Nafria, R.; Carrete, A.; Cabot, A. *Chem. Mater.* **2011**, *23*, 3095–3104.
- (106) Cabot, A.; Ibáñez, M.; Guardia, P.; Alivisatos, A. J. *Am. Chem. Soc.* **2009**, *131*, 11326–11328.
- (107) Joo, J.; Pietryga, J. M.; McGuire, J. A.; Jeon, S.-H.; Williams, D. J.; Wang, H.-L.; Klimov, V. I. *J. Am. Chem. Soc.* **2009**, *131*, 10620–10628.
- (108) Evans, C. M.; Evans, M. E.; Krauss, T. D. *J. Am. Chem. Soc.* **2010**, *132*, 10973–10975.
- (109) Yu, K.; Hrdina, A.; Zhang, X.; Ouyang, J.; Leek, D. M.; Wu, X.; Gong, M.; Wilkinson, D.; Li, C. *Chem. Commun.* **2011**, *47*, 8811–8813.
- (110) Yu, K.; Ouyang, J.; Leek, D. M. *Small* **2011**, *7*, 2250–2262.
- (111) Alper, H.; Einstein, F. W. B.; Hartstock, F. W.; Jones, R. H. *Organometallics* **1987**, *6*, 829–833.
- (112) Voronkov, M. G.; Vyazankin, N. S.; Deryagina, E. N.; Nakhmanovich, A. S.; Usov, V. A. *Reactions of sulfur with organic compounds*; Springer: New York, 1987.
- (113) Pouliquen, F.; Blanc, C.; Arretz, E.; Labat, I.; Tournier-Lasserre, J.; Ladousse, A.; Nougayrede, J.; Savin, G.; Ivaldi, R.; Nicolas, M.; Fialaire, J.; Millischer, R.; Azema, C.; Espagno, L.; Hemmer, H.; Perrot, J. *Ullmann's encyclopedia of industrial chemistry*; Wiley-VCH: 2000.
- (114) Swanston, J. *Ullmann's encyclopedia of industrial chemistry*; Wiley-VCH: 2006.
- (115) Denk, M. K. *Eur. J. Inorg. Chem.* **2009**, 1358–1368.
- (116) Bryce, W. A.; Hinshelwood, C. J. *Am. Chem. Soc.* **1949**, 3379–3387.
- (117) Hull, C. M.; Olsen, S. R.; France, W. G. *J. Ind. Eng. Chem.* **1946**, *38*, 1282–1288.
- (118) Li, L. S.; Pradhan, N.; Wang, Y.; Peng, X. *Nano Lett.* **2004**, *4*, 2261–2264.
- (119) Zhong, X.; Feng, Y.; Knoll, W.; Han, M. J. *Am. Chem. Soc.* **2003**, *125*, 13559–13563.
- (120) Bae, W. K.; Nam, M. K.; Char, K.; Lee, S. *Chem. Mater.* **2008**, *20*, 5307–5313.
- (121) Yordanov, G. G.; Yoshimura, H.; Dushkin, C. D. *Colloid Polym. Sci.* **2008**, *286*, 813–817.
- (122) Li, Z.; Ji, Y.-J.; Xie, R.; Grisham, S. Y.; Peng, X.-G. *J. Am. Chem. Soc.* **2011**, *133*, 17248–17256.
- (123) Cao, Y. C.; Wang, J. J. *Am. Chem. Soc.* **2004**, *126*, 14336–14337.
- (124) Ouyang, J.; Kuijper, J.; Brot, S.; Kingston, D.; Wu, X.; Leek, D. M.; Hu, M. Z.; Ripmeester, J. A.; Yu, K. *J. Phys. Chem. C* **2009**, *113*, 7579–7593.
- (125) Coran, A. Y. *J. Appl. Polym. Sci.* **2003**, *87*, 24–30.
- (126) Yang, Y. A.; Wu, H.; Williams, K. R.; Cao, Y. C. *Angew. Chem., Int. Ed.* **2005**, *44*, 6712–6715.
- (127) Liu, L.; Zhuang, Z.; Xie, T.; Wang, Y.-G.; Li, J.; Peng, Q.; Li, Y. *J. Am. Chem. Soc.* **2009**, *131*, 16423–16429.
- (128) Shen, H.; Wang, H.; Li, X.; Niu, J. Z.; Wang, H.; Chen, X.; Li, L. S. *Dalton Trans.* **2009**, 10534–10540.
- (129) Ithurria, S.; Dubertret, B. *J. Am. Chem. Soc.* **2008**, *130*, 16504–16505.
- (130) Ithurria, S.; Bousquet, G.; Dubertret, B. *J. Am. Chem. Soc.* **2011**, *133*, 3070–3077.
- (131) Ouyang, J.; Zaman, M. B.; Yan, F. J.; Johnston, D.; Li, G.; Wu, X.; Leek, D.; Ratcliffe, C. I.; Ripmeester, J. A.; Yu, K. *J. Phys. Chem. C* **2008**, *112*, 13805–13811.
- (132) Yu, K.; Ouyang, J.; Zaman, M. B.; Johnston, D.; Yan, F. J.; Li, G.; Ratcliffe, C. I.; Leek, D. M.; Wu, X.; Stupak, J.; Jakubek, Z.; Whitfield, D. *J. Phys. Chem. C* **2009**, *113*, 3390–3401.
- (133) Wuyts, H.; Stewart, A. *Bull. Belg. Soc. Chim.* **1909**, *23*, 9–11.
- (134) Deng, Z.; Cao, L.; Tang, F.; Zou, B. *J. Phys. Chem. B* **2005**, *109*, 16671–16675.



- (135) Bullen, C.; van, E. J.; Jasieniak, J.; Cosgriff, J. E.; Mulder, R. J.; Rizzardo, E.; Gu, M.; Raston, C. L. *Chem. Mater.* **2010**, *22*, 4135–4143.
- (136) Davis, R. E.; Nakshbendi, H. F. *J. Am. Chem. Soc.* **1962**, *84*, 2085–2090.
- (137) Levi, T. G. *Gazz. Chim. Ital.* **1930**, *60*, 975–987.
- (138) Levi, T. G. *Gazz. Chim. Ital.* **1931**, *61*, 286–293.
- (139) Thomson, J. W.; Nagashima, K.; Macdonald, P. M.; Ozin, G. A. *J. Am. Chem. Soc.* **2011**, *133*, S036–S041.
- (140) Joo, J.; Na, H. B.; Yu, T.; Yu, J. H.; Kim, Y. W.; Wu, F.; Zhang, J. Z.; Hyeon, T. *J. Am. Chem. Soc.* **2003**, *125*, 11100–11105.
- (141) Rossetti, R.; Ellison, J. L.; Gibson, J. M.; Brus, L. E. *J. Chem. Phys.* **1984**, *80*, 4464–4469.
- (142) Wang, X.; Zhuang, J.; Peng, Q.; Li, Y. *Nature* **2005**, *437*, 121–124.
- (143) Zhang, H.; Hyun, B.-R.; Wise, F. W.; Robinson, R. D. *Nano Lett.* **2012**, *12*, 5856–5860.
- (144) Greenwood, N. N.; Earnshaw, A. *Chemistry of the elements*; Elsevier: 1997.
- (145) Maity, A. C. *Synlett* **2008**, *3*, 465–466.
- (146) Chen, O.; Chen, X.; Yang, Y.; Lynch, J.; Wu, H.; Zhuang, J.; Cao, Y. C. *Angew. Chem., Int. Ed.* **2008**, *47*, 8638–8641.
- (147) Shen, H.; Niu, J. Z.; Wang, H.; Li, X.; Li, L. S.; Chen, X. *Dalton Trans.* **2010**, *39*, 11432–11438.
- (148) Medarde, M.; Lopez, J.-L.; Iribar, J.; San, F. A.; Carpy, A.; Leger, J.-M. *Tetrahedron* **1995**, *51*, 11011–11020.
- (149) Shibuya, K. *Synth. Commun.* **1994**, *24*, 2923–2941.
- (150) Arigoni, D.; Vasella, A.; Sharpless, K. B.; Jensen, H. P. *J. Am. Chem. Soc.* **1973**, *95*, 7917–7919.
- (151) Paulmier, C. *Selenium reagents and intermediates in organic synthesis*; Pergamon: 1986.
- (152) Waitkins, G. R.; Clark, C. W. *Chem. Rev.* **1945**, *36*, 235–289.
- (153) Rabjohn, N. *Org. React.* **1976**, *24*, 261–415.
- (154) Hwu, J. R.; Wong, F. F.; Shiao, M. J. *J. Org. Chem.* **1992**, *57*, 5254–5255.
- (155) Capperucci, A.; Degl'Innocenti, A.; Funicello, M.; Mauriello, G.; Scafato, P.; Spagnolo, P. *J. Org. Chem.* **1995**, *60*, 2254–2256.
- (156) Detty, M. R.; Seidler, M. D. *J. Org. Chem.* **1982**, *47*, 1354–1356.
- (157) Segi, M.; Nakajima, T.; Suga, S.; Murai, S.; Ryu, I.; Ogawa, A.; Sonoda, N. *J. Am. Chem. Soc.* **1988**, *110*, 1976–1978.
- (158) Degl'Innocenti, A.; Capperucci, A. *Eur. J. Org. Chem.* **2000**, 2171–2186.
- (159) Capperucci, A.; Degl'Innocenti, A.; Ricci, A.; Mordini, A.; Reginato, G. *J. Org. Chem.* **1991**, *56*, 7323–7328.
- (160) Smith, D. C.; Lee, S. W.; Fuchs, P. L. *J. Org. Chem.* **1994**, *59*, 348–354.
- (161) DeGroot, M. W.; Corrigan, J. F. *Z. Anorg. Allg. Chem.* **2006**, *632*, 19–29.
- (162) Degroot, M. W.; Corrigan, J. F. In *Comprehensive coordination chemistry II*; McCleverty, J. A., Meyer, T. J., Eds.; Pergamon: Oxford, 2003; pp 57–123.
- (163) MacDonald, D. G.; Corrigan, J. F. *Philos. Trans. R. Soc. A* **2010**, *368*, 1455–1472.
- (164) Abel, E. W. *J. Chem. Soc.* **1961**, 4933–4935.
- (165) So, J. H.; Boudjouk, P. *Synthesis* **1989**, *4*, 306–307.
- (166) Harpp, D. N.; Steliou, K. *Synthesis* **1976**, *11*, 721–722.
- (167) Schmidt, M.; Ruf, H. Z. *Anorg. Allg. Chem.* **1963**, *321*, 270–273.
- (168) Buerger, H.; Goetze, U. *Inorg. Nucl. Chem. Lett.* **1967**, *3*, 549–552.
- (169) Syper, L.; Mlochowski, J. *Tetrahedron* **1988**, *44*, 6119–6130.
- (170) Emin, S. M.; Dushkin, C. D.; Nakabayashi, S.; Adachi, E. *Cent. Eur. J. Chem.* **2007**, *5*, 590–604.
- (171) Ogawa, A.; Sonoda, N. In *Handbook of reagents for organic synthesis: Reagents for silicon-mediated organic synthesis*; Fuchs, P. L., Ed.; John Wiley & Sons: 2001; pp 82–83.
- (172) Hooton, K. A.; Allred, A. L. *Inorg. Chem.* **1965**, *4*, 671–678.
- (173) Turner, E. A.; Roesner, H.; Huang, Y.; Corrigan, J. F. *J. Phys. Chem. C* **2007**, *111*, 7319–7329.
- (174) DeGroot, M. W.; Corrigan, J. F. *Organometallics* **2005**, *24*, 3378–3385.
- (175) Tran, D. T. T.; Corrigan, J. F. *Organometallics* **2000**, *19*, S202–S208.
- (176) DeGroot, M. W.; Taylor, N. J.; Corrigan, J. F. *Inorg. Chem.* **2005**, *44*, S447–S458.
- (177) Bunge, S. D.; Krueger, K. M.; Boyle, T. J.; Rodriguez, M. A.; Headley, T. J.; Colvin, V. L. *J. Mater. Chem.* **2003**, *13*, 1705–1709.
- (178) Li, M.; Ouyang, J.; Ratcliffe, C. I.; Pietri, L.; Wu, X.; Leek, D. M.; Moudrakovski, I.; Lin, Q.; Yang, B.; Yu, K. *ACS Nano* **2009**, *3*, 3832–3838.
- (179) Peng, X.; Schlamp, M. C.; Kadavanich, A. V.; Alivisatos, A. P. *J. Am. Chem. Soc.* **1997**, *119*, 7019–7029.
- (180) Hines, M. A.; Guyot-Sionnest, P. *J. Phys. Chem.* **1996**, *100*, 468–471.
- (181) Jung, S. I.; Yeo, H. Y.; Yun, I.; Cho, S. M.; Han, I. K.; Lee, J. I. *J. Nanosci. Nanotechnol.* **2008**, *8*, 4899–4902.
- (182) Dabbousi, B. O.; Rodriguez-Viejo, J.; Mikulec, F. V.; Heine, J. R.; Mattoussi, H.; Ober, R.; Jensen, K. F.; Bawendi, M. G. *J. Phys. Chem. B* **1997**, *101*, 9463–9475.
- (183) Santra, P. K.; Viswanatha, R.; Daniels, S. M.; Pickett, N. L.; Smith, J. M.; O'Brien, P.; Sarma, D. D. *J. Am. Chem. Soc.* **2009**, *131*, 470–477.
- (184) Kortan, A. R.; Hull, R.; Opila, R. L.; Bawendi, M. G.; Steigerwald, M. L.; Carroll, P. J.; Brus, L. E. *J. Am. Chem. Soc.* **1990**, *112*, 1327–1332.
- (185) Hines, M. A.; Scholes, G. D. *Adv. Mater.* **2003**, *15*, 1844–1849.
- (186) Liu, T.-Y.; Li, M.; Ouyang, J.; Zaman, M. B.; Wang, R.; Wu, X.; Yeh, C.-S.; Lin, Q.; Yang, B.; Yu, K. *J. Phys. Chem. C* **2009**, *113*, 2301–2308.
- (187) Lee, J.-S.; Shevchenko, E. V.; Talapin, D. V. *J. Am. Chem. Soc.* **2008**, *130*, 9673–9675.
- (188) Abel, K. A.; Shan, J.; Boyer, J.-C.; Harris, F.; van Veggel, F. C. J. M. *Chem. Mater.* **2008**, *20*, 3794–3796.
- (189) Smith, D. K.; Luther, J. M.; Semonin, O. E.; Nozik, A. J.; Beard, M. C. *ACS Nano* **2011**, *5*, 183–190.
- (190) Marcotrigiano, G.; Peyronel, G.; Battistuzzi, R. *J. Chem. Soc., Perkin Trans. 2* **1972**, 1539–1541.
- (191) Bordwell, F. G.; Ji, G. Z. *J. Am. Chem. Soc.* **1991**, *113*, 8398–8401.
- (192) Walter, J. L.; Ryan, J. A.; Lane, T. J. *J. Am. Chem. Soc.* **1956**, *78*, 5560–5562.
- (193) Warner, R. C. *J. Biol. Chem.* **1942**, *142*, 705–723.
- (194) Buchanan, G. H.; Barsky, G. J. *J. Am. Chem. Soc.* **1930**, *52*, 195–206.
- (195) Zhou, Y.; Denk, M. K. *Tetrahedron Lett.* **2003**, *44*, 1295–1299.
- (196) Batey, R. A.; Powell, D. A. *Org. Lett.* **2000**, *2*, 3237–3240.
- (197) Fathalla, W.; Cajan, M.; Marek, J.; Pazdera, P. *Molecules* **2001**, *6*, 588–602.
- (198) Aly, A. A.; Ahmed, E. K.; El-Mokadem, K. M.; Hegazy, M. E.-A. *J. Sulfur Chem.* **2007**, *28*, 73–93.
- (199) Fernandez-Bolanos, J. G.; Lopez, O.; Ulgar, V.; Maya, I.; Fuentes, J. *Tetrahedron Lett.* **2004**, *45*, 4081–4084.
- (200) Koketsu, M.; Suzuki, N.; Ishihara, H. *J. Org. Chem.* **1999**, *64*, 6473–6475.
- (201) Keil, D.; Hartmann, H. *Synthesis* **2004**, *1*, 15–16.
- (202) Maeda, H.; Takashima, M.; Sakata, K.; Watanabe, T.; Honda, M.; Segi, M. *Tetrahedron Lett.* **2011**, *52*, 415–417.
- (203) Andaloussi, M. B. D.; Mohr, F. J. *Organomet. Chem.* **2010**, *695*, 1276–1280.
- (204) Koketsu, M.; Takakura, N.; Ishihara, H. *Synth. Commun.* **2002**, *32*, 3075–3079.
- (205) Koketsu, M.; Fukuta, Y.; Ishihara, H. *J. Org. Chem.* **2002**, *67*, 1008–1011.
- (206) Yavari, I.; Hosseini, N.; Moradi, L.; Mirzaei, A. *Tetrahedron Lett.* **2008**, *49*, 4239–4241.

- (207) Koketsu, M.; Fukuta, Y.; Ishihara, H. *Tetrahedron Lett.* **2001**, 42, 6333–6335.
- (208) Minoura, M.; Kawashima, T.; Okazaki, R. *Tetrahedron Lett.* **1997**, 38, 2501–2504.
- (209) Lappert, M. F.; Martin, T. R.; McLaughlin, G. M. *J. Chem. Soc., Chem. Commun.* **1980**, 635–637.
- (210) Yu, S.-H.; Yang, J.; Han, Z.-H.; Zhou, Y.; Yang, R.-Y.; Qian, Y.-T.; Zhang, Y.-H. *J. Mater. Chem.* **1999**, 9, 1283–1287.
- (211) Yang, J.; Zeng, J.-H.; Yu, S.-H.; Yang, L.; Zhou, G.-e.; Qian, Y.-t. *Chem. Mater.* **2000**, 12, 3259–3263.
- (212) Yang, J.; Xue, C.; Yu, S.-H.; Zeng, J.-H.; Qian, Y.-T. *Angew. Chem., Int. Ed.* **2002**, 41, 4697–4700.
- (213) Zhan, J.; Yang, X.; Wang, D.; Li, S.; Xie, Y.; Xia, Y.; Qian, Y. *Adv. Mater.* **2000**, 12, 1348–1357.
- (214) Yu, S.-H.; Yoshimura, M.; Moreno, J. M. C.; Fujiwara, T.; Fujino, T.; Teranishi, R. *Langmuir* **2001**, 17, 1700–1707.
- (215) Jang, J. S.; Joshi, U. A.; Lee, J. S. *J. Phys. Chem. C* **2007**, 111, 13280–13287.
- (216) Kar, S.; Santra, S.; Heinrich, H. *J. Phys. Chem. C* **2008**, 112, 4036–4041.
- (217) Gu, Z.; Zou, L.; Fang, Z.; Zhu, W.; Zhong, X. *Nanotechnology* **2008**, 19, 135604-1–135604-7.
- (218) Yu, S.-H.; Yoshimura, M. *Adv. Mater.* **2002**, 14, 296–300.
- (219) Chen, X.; Xu, H.; Xu, N.; Zhao, F.; Lin, W.; Lin, G.; Fu, Y.; Huang, Z.; Wang, H.; Wu, M. *Inorg. Chem.* **2003**, 42, 3100–3106.
- (220) Zhao, Q.; Hou, L.; Huang, R. *Inorg. Chem. Commun.* **2003**, 6, 971–973.
- (221) Yao, W.-T.; Yu, S.-H.; Wu, Q.-S. *Adv. Funct. Mater.* **2007**, 17, 623–631.
- (222) Fang, Z.; Li, Y.; Zhang, H.; Zhong, X.; Zhu, L. *J. Phys. Chem. C* **2009**, 113, 14145–14150.
- (223) Chung, J.; Myoung, J.; Oh, J.; Lim, S. *J. Phys. Chem. C* **2010**, 114, 21360–21365.
- (224) Geng, J.; Liu, B.; Xu, L.; Hu, F.-N.; Zhu, J.-J. *Langmuir* **2007**, 23, 10286–10293.
- (225) Gao, T.; Li, Q.; Wang, T. *Chem. Mater.* **2005**, 17, 887–892.
- (226) Arul, D. N.; Gedanken, A. *Appl. Phys. Lett.* **1998**, 72, 2514–2516.
- (227) Wang, C.; Zhang, H.; Zhang, J.; Li, M.; Sun, H.; Yang, B. *J. Phys. Chem. C* **2007**, 111, 2465–2469.
- (228) Zhu, J.; Koltypin, Y.; Gedanken, A. *Chem. Mater.* **2000**, 12, 73–78.
- (229) Wada, Y.; Kuramoto, H.; Anand, J.; Kitamura, T.; Sakata, T.; Mori, H.; Yanagida, S. *J. Mater. Chem.* **2001**, 11, 1936–1940.
- (230) Karan, S.; Mallik, B. *J. Phys. Chem. C* **2007**, 111, 16734–16741.
- (231) Panda, A. B.; Glaspell, G.; El-Shall, M. S. *J. Am. Chem. Soc.* **2006**, 128, 2790–2791.
- (232) Pan, D.; Jiang, S.; An, L.; Jiang, B. *Adv. Mater.* **2004**, 16, 982–985.
- (233) Pan, D.; Wang, Q.; Jiang, S.; Ji, X.; An, L. *Adv. Mater.* **2005**, 17, 176–179.
- (234) Wang, Q.; Pan, D.; Jiang, S.; Ji, X.; An, L.; Jiang, B. *Chem.—Eur. J.* **2005**, 11, 3843–3848.
- (235) Pan, D.; Wang, Q.; Jiang, S.; Ji, X.; An, L. *J. Phys. Chem. C* **2007**, 111, 5661–5666.
- (236) Pan, D.; Wang, Q.; Pang, J.; Jiang, S.; Ji, X.; An, L. *Chem. Mater.* **2006**, 18, 4253–4258.
- (237) Zhao, Y.; Zhang, Y.; Zhu, H.; Hadjipanayis, G. C.; Xiao, J. Q. *J. Am. Chem. Soc.* **2004**, 126, 6874–6875.
- (238) Dawood, F.; Schaak, R. E. *J. Am. Chem. Soc.* **2009**, 131, 424–425.
- (239) Artemyev, M. V.; Bibik, A. I.; Gurinovich, L. I.; Gaponenko, S. V.; Woggon, U. *Phys. Rev. B* **1999**, 60, 1504–1506.
- (240) Artemyev, M. V.; Woggon, U.; Jaschinski, H.; Gurinovich, L. I.; Gaponenko, S. V. *J. Phys. Chem. B* **2000**, 104, 11617–11621.
- (241) Panda, A. B.; Acharya, S.; Efrima, S. *Adv. Mater.* **2005**, 17, 2471–2474.
- (242) Panda, A. B.; Acharya, S.; Efrima, S.; Golan, Y. *Langmuir* **2007**, 23, 765–770.
- (243) Acharya, S.; Sarma, D. D.; Jana, N. R.; Pradhan, N. *J. Phys. Chem. Lett.* **2010**, 1, 485–488.
- (244) Pradhan, N.; Xu, H.; Peng, X. *Nano Lett.* **2006**, 6, 720–724.
- (245) Liu, Y.-H.; Wayman, V. L.; Gibbons, P. C.; Loomis, R. A.; Buhro, W. E. *Nano Lett.* **2010**, 10, 352–357.
- (246) Chae, W.-S.; Shin, H.-W.; Lee, E.-S.; Shin, E.-J.; Jung, J.-S.; Kim, Y.-R. *J. Phys. Chem. B* **2005**, 109, 6204–6209.
- (247) Dhas, N. A.; Zaban, A.; Gedanken, A. *Chem. Mater.* **1999**, 11, 806–813.
- (248) Joo, J.; Son, J. S.; Kwon, S. G.; Yu, J. H.; Hyeon, T. *J. Am. Chem. Soc.* **2006**, 128, 5632–5633.
- (249) Bouroushian, M. *Electrochemistry of metal chalcogenides*; Springer: Berlin, 2010.
- (250) Pietikainen, J.; Laitinen, R. S. *Chem. Commun.* **1998**, 2381–2382.
- (251) Smith, D. M.; Ibers, J. A. *Coord. Chem. Rev.* **2000**, 200–202, 187–205.
- (252) Li, Y.; Jing, L.; Qiao, R.; Gao, M. *Chem. Commun.* **2011**, 47, 9293–9311.
- (253) Resch, U.; Weller, H.; Henglein, A. *Langmuir* **1989**, 5, 1015–1020.
- (254) Mandal, A.; Tamai, N. *J. Phys. Chem. C* **2008**, 112, 8244–8250.
- (255) Xu, S.; Wang, C.; Xu, Q.; Zhang, H.; Li, R.; Shao, H.; Lei, W.; Cui, Y. *Chem. Mater.* **2010**, 22, 5838–5844.
- (256) Yang, W.-h.; Li, W.-w.; Dou, H.-j.; Sun, K. *Mater. Lett.* **2008**, 62, 2564–2566.
- (257) Zhang, J.; Jin, S.; Fry, H. C.; Peng, S.; Shevchenko, E.; Wiederrecht, G. P.; Rajh, T. *J. Am. Chem. Soc.* **2011**, 133, 15324–15327.
- (258) Son, J.-S.; Yu, J.-H.; Kwon, S.-G.; Lee, J.-H.; Joo, J.; Hyeon, T.-H. *Adv. Mater.* **2011**, 23, 3214–3219.
- (259) Shen, H.; Wang, H.; Chen, X.; Niu, J. Z.; Xu, W.; Li, X. M.; Jiang, X.-D.; Du, Z.; Li, L. S. *Chem. Mater.* **2010**, 22, 4756–4761.